AD-A091 891 ROYAL AIRCRAFT ESTABLISHMENT FARNBOROUGH (ENGLAND) F/G 20/4
FLOW MEASUREMENTS IN THE WAKE OF A WING FITTED WITH A LEADING-E--ETC(U)
SEP 79 P J BUTTERWORTH
UNCLASSIFIED RAE-TR-79120 DRIC-BR-72779 NL

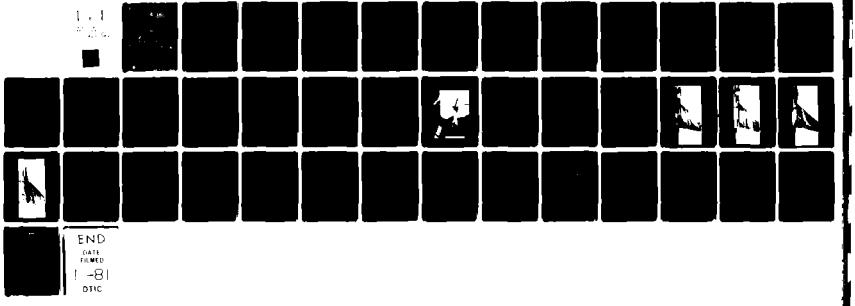

END
DATE FILMED
-81
DTIC

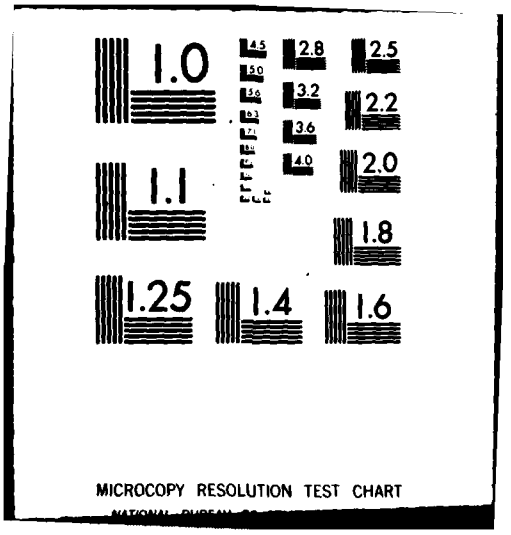
1.0
1.1
1.25
1.4
1.6
1.8
2.0
2.2
2.5
2.8
3.2
3.6
4.0
4.5
5.0
5.6
6.3
7.1
8.0
9.0
MICROCOPY RESOLUTION TEST CHART

LEVEL II

ROYAL AIRCRAFT ESTABLISHMENT

* RAE-TR-

Technical Report 79120

RAE AERO-3[illegible]

(11) Sept[illegible]79

(12) 42

# FLOW MEASUREMENTS IN THE WAKE OF A WING FITTED WITH A LEADING-EDGE BOOT EXTENSION (STRAKE).

technical rept.

by

(10) P.J. Butterworth



*

Procurement Executive, Ministry of Defence
Farnborough, Hants

320450

UDC 533.693.5 : 533.693 : 533.691.1 : 533.6.048.3 : 533.6.08

ROYAL AIRCRAFT ESTABLISHMENT

Technical Report 79120

Received for printing 11 September 1979

# FLOW MEASUREMENTS IN THE WAKE OF A WING FITTED WITH A LEADING-EDGE ROOT EXTENSION (STRAKE)

by

P. J. Butterworth

## SUMMARY

In a low-speed wind tunnel measurements have been taken of the velocity vector in the flow field behind the wing of a combat aircraft model. The wing was fitted with a leading-edge root extension (strake) and could have either a plain leading edge or a deployed slat outboard. Four flow investigations were made; at three angles of incidence with the plain leading edge and at one angle of incidence with the slat deployed.

The data from each of these tests have been analysed to give the distribution of the total head deficit, the streamwise component of vorticity and a measure of the circulation distribution in the wake of the wing.

Departmental Reference: Aero 3464

## LIST OF CONTENTS

## 1 INTRODUCTION

To meet the present day requirement for a rapid manoeuvre capability a strike-fighter aircraft has to be able to 'keep flying' over a wide range of attitudes and speed. There has consequently been a new emphasis on the development of variable and fixed-geometry devices which extend the usable range of incidence of swept-wing aircraft throughout the subsonic speed range.

One fixed-geometry device which is being adopted is the leading-edge root extension or strake which has the advantage of adding some of the beneficial effects of the characteristics of slender wings to the conventional swept wing shape. The types of flow associated with this hybrid design are complex since 'conventional' swept-wing flow may still be present over the outboard wing but inboard the effect of the strong vortex flow associated with the highly swept sharp-edged strake is dominant. Thus at incidences where the wing without the strake would have been completely stalled, this strake vortex dominates the flow over much of the wing and only the flow over the outboard part is stalled; the generation of lift is thus maintained to higher incidences than would be the case for the wing alone[1]. In order to aid the design of efficient wing/strake configurations, the associated complex mixed flows need to be well understood. The work described in this Report is intended to assist this understanding and consists of detailed flow surveys of the wake of such a configuration.

The work was done using a combat aircraft model on which extensive force and moment measurements have been made, for a number of strake configurations, in the 13 ft × 9 ft low-speed wind tunnel at RAE Bedford[1,2]. For the flow surveys, the model was tested in the No.2 11½ ft × 8½ ft low-speed wind tunnel at RAE Farnborough. Using an automatic wake traverse gear, a large number of measurements was taken to determine the velocity vector in the flow field behind the wing fitted with a sharp-edged delta strake having a leading-edge sweep of 75° (*ie* Strake 2 of Ref 1).

From these measurements, the distributions of the total head deficit, the streamwise component of vorticity and the circulation in the wake were derived and the results are described in this Report. In Maskell's analysis[3] the determination of the first two of these quantities is the first step towards evaluating the profile drag and the lift and vortex drag of the wing. It would also be possible to derive distributions of downwash, sidewash or static pressure in the wake but this has not been done since it is believed that they would offer little extra to the understanding of the complex type of flow.

## 2 MODEL AND TEST DETAILS

### 2.1 Model details

The general arrangement of the model is shown in Fig 1 and the principal dimensions are given in Table 1. The wing is of nominal aspect ratio 3.0. It has a leading-edge sweep angle of $40^{\circ}$ and a streamwise thickness/chord ratio of 0.08. Further details of the model are given in Ref 1.

Of the different strakes reported in Ref 1, the one which was chosen for this investigation was Strake 2 which has a delta planform with a $75^{\circ}$ swept leading edge. It is not cambered and has a sharp leading-edge profile. This strake was chosen because, of those tested, it has the maximum ratio of increase in maximum lift coefficient to strake planform area.

The model can be fitted either with a plain leading edge (Fig 1 port side) or a leading-edge slat (Fig 1 starboard side) and tests were made with both these configurations. Outboard of the strake, the leading-edge slat has a local chord of 0.18c (where c is the local wing chord) and it is deployed in the streamwise direction with a deflection of $25^{\circ}$. When deployed, it is supported by three brackets the positions of which are shown in Fig 1. Fig 2 shows the model rigged in the No.2 11½ ft × 8½ ft low-speed wind tunnel with the slats deployed.

Fig 2 also shows how the model was mounted in the tunnel (on the underfloor, virtual centre, mechanical balance). There was a main support strut attached to the lower surface of each wing at about two-thirds semispan and the angle of incidence was controlled by a strut attached to the underside of the afterbody. To prevent excessive compression loads in this incidence strut, a counterbalance weight was suspended under the tunnel floor by a wire fixed to the underside of the body near the nose.

### 2.2 Test details and analysis

To confirm the results of Refs 1 and 2, the longitudinal forces and moments were measured on the model for both the leading-edge configurations considered in this investigation. The longitudinal characteristics discussed in section 3.1 are taken from Refs 1 and 2 since they include results for a configuration without a strake. However, for both the configurations which were tested the differences between the results from the two tunnels are small.

For the flow-field investigations, the local velocity vector and total head deficit were determined at a large number of points (Table 2) in a plane normal to the tunnel centreline 120 mm downstream of the wing tip.

Measurements were made behind the starboard wing using the wake traverse gear which can be seen in Fig 2 downstream of the model and which is described in Ref 4. To check any possible interference between the model and the traverse gear (either aerodynamic or mechanical) the longitudinal forces and moments were monitored throughout the flow-field investigations.

For the model configuration with a plain leading edge outboard of the strake, flow-field measurements were made for three geometric angles of incidence:

(i) a low value of $7^{\circ}$ where the wing experiences attached flow outboard and vortex-dominated flow inboard;

(ii) a moderate value of $14^{\circ}$ close to a kink in the lift curve[1] and approaching the incidence at which the lift break occurs for the wing alone;

(iii) a high value of $25^{\circ}$ close to that at which maximum lift is generated.

For the configuration with the slat deployed outboard of the strake, the flow field was investigated at an incidence of $14^{\circ}$ for comparison with (ii) above. The nominal wind speed for these flow investigations was 50 m $s^{-1}$ giving a Reynolds number of $1.72 \times 10^{6}$ based on the standard mean chord of 0.505 m.

The raw data output by the traverse gear instrumentation was reduced using the suite of computer programs described in Refs 4 and 5. At each point of the traverse, the local downwash and sidewash, total head deficit, static pressure coefficient and the total velocity and its three components were calculated. Other programs in the suite[5] which were written to provide data for Maskell's method of analysis[3] were used to calculate the streamwise component of vorticity at the centre of each small square of the measuring grid - positive vorticity representing rotation in an anticlockwise sense looking upstream. From all this information, distributions of total head deficit, $(H - H_0)/q_0$ and streamwise component of vorticity, $\xi\bar{c}/U_0$, in the wake were initially selected for presentation in this Report.

The distributions of the streamwise component of vorticity, Figs 8, 11, 15 and 18, show distinct regions of positive and negative vorticity. The non-dimensionalised circulation, $\Gamma/U_0\bar{c}$, has been evaluated for these regions by numerical integration of the tangential velocity components around the boundaries; where necessary the regions were closed by drawing appropriate approximate boundaries. These values of the circulation are shown in summary figures, Figs 9, 12, 16 and 19, which also show the spanwise distribution of circulation $\Gamma(Y)/U_0\bar{c}$, in the narrow wake behind the wing.

One further experiment was done to determine the trajectory of the core of the strake vortex for the configuration with the plain leading edge at an incidence of 14°. To avoid any interference, either aerodynamic or mechanical, for this test the normal quadrant-mounted, self-aligning head of the traverse gear had to be replaced by a longer four-tube yawmeter which could not be aligned with the local flow. However, by reading the pressure differences across opposing pairs of tubes as the head was traversed in a plane normal to the freestream, a point in the vortex was defined where the downwash and sidewash were zero. Repetition of this procedure in planes up-and downstream of the main traverse plane enabled the approximate trajectory of the strake vortex to be found. (It is only approximate since the trajectory of the strake vortex is not streamwise and therefore the locus defined for the point of zero downwash and sidewash is not in general the centre of the vortex core. However, the differences between this locus and the core centre are likely to be small and can be neglected.)

## 3 RESULTS FROM TESTS IN THE 13 ft × 9 ft TUNNEL

Before we examine the results of the detailed flow measurements made in the No.2 11½ ft × 8½ ft tunnel, it is worth considering the force and flow visualisation data obtained earlier[1,2] which demonstrated the need for further work.

### 3.1 Longitudinal force and moment characteristics

The determination of the longitudinal force characteristics of the model was not one of the primary aims of this investigation since it has been reported elsewhere[1,2]. However a brief listing of the major effects of adding the strake and deploying the slat is useful for completeness and therefore follows. (The results are taken from Refs 1 and 2.)

The lift, drag and pitching moment curves (corrected for tunnel constraint and blockage) in Figs 3, 4 and 5 respectively show that the addition of the strake has the following effects:

(i) the lift curve slope is increased marginally at $\alpha$ greater than approximately 10° and substantial lift continues to be generated beyond the incidence at which the lift break occurs for the wing alone (≈16.5°);

(ii) the drag of the model is increased below the incidence for the lift break for the wing alone but is significantly decreased above this incidence;

(iii) there is an increase in nose-up pitching moment; this is to be expected with the addition of wing area forward of the moment centre.

The kink in the lift curve for the configuration of wing with plain leading edge and strake (mentioned briefly in section 2.2) can be seen in Fig 3 at an incidence just less than that at which the lift break occurs for the wing alone.

The effects of deploying the slat on the wing/strake configuration are:

(i) a reduction in $C_L$ for incidences less than $27^o$ but a continued increase in $C_L$ beyond that incidence, Fig 3;

(ii) increased values of $C_D$ for values of $C_L < 0.9$ but decreased for higher values of $C_L$, Fig 4;

(iii) only minor changes in the longitudinal stability characteristics, Fig 5 (except at the highest incidences).

3.2 Surface flow patterns

Fig 6a-c show surface flow-visualisation patterns on the upper surface of the wing with the plain leading edge and strake at geometric incidences of $10^o$, $14^o$ and $22^o$ (taken from Ref 1). At an incidence of $10^o$, Fig 6a (which is typical of low incidence flow patterns) the strake vortex is seen to be swept downstream over the inboard part of the main wing - it does not appear to influence the flow on the outboard part of the wing where the flow is approximately streamwise.

At an incidence of $14^o$, Fig 6b, the flow on the outboard part of the wing upper surface has a significant component of sidewash although the strake vortex is apparently still being swept downstream across the inboard part of the wing. Near $14^o$ of incidence, the lift break occurs for the wing alone and there is a kink in the lift curve for the wing/strake combination (see Fig 3). Evidently, $14^o$ is in some sense a transitional incidence between the type of flow shown in Fig 6a ($\alpha_g \approx 10^o$) and that in Fig 6c ($\alpha_g \approx 22^o$).

At an incidence of $22^o$, Fig 6c shows that the entire upper surface of the wing is affected by the strake vortex although the flow pattern on the forward part of the outboard wing is not dis-similar to that expected on a stalled swept wing without a strake. Since this type of flow persists to the maximum point of the lift curve, it was decided to do a traverse at as high an incidence as possible. Buffeting of the model in the tunnel restricted this incidence to $25^o$.

Fig 6d shows the flow pattern on the wing at an incidence of $14^{o}$ for the configuration with the leading-edge slat deployed (taken from Ref 2). The slat is seen to prevent flow separation on the outboard wing and the sidewash in this region is much reduced compared with that shown in Fig 6b for the plain leading edge.

## 4 WAKE SURVEY RESULTS

This section is divided into four subsections, each one discussing the results of a single survey. The incidences at which the surveys were made are quoted as geometric incidences, *ie* they are not corrected for wind-tunnel wall constraint. This has been done because the survey plane is normal to the tunnel centreline not to the constrained stream vector.

### 4.1 $\alpha_g = 7^{o}$, plain leading edge

Fig 7 shows the distribution of total head deficit, $(H - H_0)/q_0$ , in the wake of the wing/strake configuration at a geometric incidence $\alpha_g = 7^{o}$ .

This figure shows that there is a region of deficit extending outboard from the body side (at $Y \approx 100$ mm) to $Y \approx 280$ mm which is apparently typical of that in the wake of a swept wing with attached flow. However in the range $280 \text{ mm} \leq Y \leq 400$ mm there is, in addition, a region of deficit above the wing trailing edge associated with the strake primary vortex. Further outboard there is again a normal swept wing attached-flow wake but near $Y = 500$ mm , there is a spur extending downwards which defines the wake from the main support strut on the wing. The attached-flow wake extends outboard to where the region of deficit due to the tip vortex is visible. It should be noted that this tip vortex region has two local minima; a possible explanation for this is given later.

The distribution of the streamwise component of vorticity, $\xi\bar{c}/U_0$ , is shown in Fig 8. As may be seen, the region within which the vorticity is confined corresponds closely with the contour for the lowest total head deficit drawn in Fig 7 (-0.005).

The wake behind the inboard part of the wing ($Y < 280$ mm) has negative (*ie* clockwise) values of $\xi\bar{c}/U_0$ due to the outwash induced on the upper surface of the wing by the strake primary vortex. This narrow wake continues into the region defined by $280 \text{ mm} \leq Y \leq 400$ mm which shows three interesting features:

(i) large positive values of $\xi\bar{c}/U_0$ in the strake primary vortex (up to 30);

(ii) a region of relatively large negative values ($\xi\bar{c}/U_0$ as low as -15) just below and outboard of the centre of the primary vortex;

(iii) extending from (ii) above a narrow tongue of weak negative vorticity.

The position of the negative vorticity to which attention is drawn in (ii) above suggests that like the narrow wake inboard, it too is induced by the strake primary vortex. The strake secondary vortex which is visible in the surface flow pattern on the strake in Fig 6a has negative values of vorticity and could be the origin of the narrow tongue of weak negative vorticity referred to in (iii) above.

In the outboard region ($Y \geq 400$ mm) the attached-flow part of the wake has the positive values of $\xi\bar{c}/U_0$ which would be expected behind a conventional swept wing suggesting that the effect of the strake vortex is small in this region. In the tip vortex region there is a very high value of $\xi\bar{c}/U_0$ (>100) but above this there is a weaker negative region (corresponding to the second local minimum of $(H - H_0)/q_0$ referred to above). It is assumed that this clockwise rotation (negative values of $\xi\bar{c}/U_0$) is due to a secondary vortex induced by the separation of the flow beneath the main tip vortex at or near to the square cut wing tip. There is some evidence for this interpretation in Fig 6a. It is thus possible that after the flow leaves the trailing edge of the tip, this secondary vortex is swept around the periphery of the main tip vortex and that in the plane of the wake survey it is located just above the main vortex. This suggestion can only be verified by doing further surveys closer to the wing tip and thereby tracing the origin of the small region of negative vorticity.

Fig 9 shows the distribution of circulation in the wake. The upper part of this figure defines particular regions of the survey plane which are closed, where necessary to permit analysis, along the dashed lines. The solid boundaries correspond to the zero contours of vorticity shown in Fig 8. The circulation associated with each closed region is shown on the figure. The lower part of the figure shows the spanwise distribution of circulation $\Gamma(Y)/U_0\bar{c}$, in the narrow wake for $150 \text{ mm} \leq Y \leq 760 \text{ mm}$. At any spanwise station $Y$, the value of circulation plotted is the circulation in the narrow wake outboard of that station.

### 4.2 $\alpha_g = 14^\circ$, plain leading edge

Figs 10, 11 and 12 present the distributions of total head deficit, streamwise component of vorticity and circulation in the wake for the incidence $\alpha_g = 14^\circ$.

Fig 10 shows that large changes in the distribution of the total head deficit in the wake have occurred as the incidence has been increased from $7^{\circ}$ (*cf* Fig 7). In particular, that part of the wake associated with the outboard part of the wing has expanded and no concentrated tip-vortex wake is evident. Also, the cross-sectional area of the wake of the strake primary vortex has grown.

Fig 11 shows that in the survey plane below the level of the wing trailing edge there is a band of negative vorticity ($\xi\bar{c}/U_0$) which extends right out to beyond the wing tip (*cf* Fig 8 for $\alpha_g = 7^{\circ}$ where this negative region exists only inboard of $Y = 440$ mm). The region of positive $\xi\bar{c}/U_0$ associated with the strake primary vortex has grown significantly in size although at both $\alpha_g = 7^{\circ}$ and $14^{\circ}$ the peak values of $\xi\bar{c}/U_0$ in this part of the wake are similar. This suggests that by the higher incidence the strake primary vortex has broken down upstream of the survey plane; this would be consistent with the increased area occupied by its wake[6].

The tongue of negative vorticity beside the wake of the strake primary vortex has increased in both size and strength and now appears to be more associated with the negative concentration below and slightly inboard of it. The wake outboard near the wing tip does not have the high values of $\xi\bar{c}/U_0$ in the tip vortex wake which are present for $\alpha_g = 7^{\circ}$ (Fig 8). Also, there is no evidence of a region of contra-rotating flow near the tip vortex and its absence is supported by the flow pattern shown in Fig 6b.

Once again, the contours of zero $\xi\bar{c}/U_0$ were used to define areas of the wake which were closed as necessary so that the distributon of circulation in the wake could be calculated. This distribution is shown in Fig 12. Notice particularly that $\Gamma(Y)/U_0\bar{c}$ is negative for all values of $Y$, Fig 12b.

Fig 13 shows the trajectory of the strake primary vortex relative to the model. The technique described in section 2.2 was used to locate the point within the primary vortex where the downwash and sidewash are zero. This was done at streamwise stations 60 mm apart as far forward as $X = -600$ mm (the forward limit of the probe movement) and as far aft as $X = 600$ mm. Because of the flexibility of the necessarily long probe and the strength of the flow field in which it was used, the windspeed had to be reduced to 40 m $s^{-1}$ ($R = 1.38 \times 10^6$) for this test. As shown in the top half of Fig 13 the trajectory of the strake primary vortex can be linearly extrapolated to the apex of the strake.

## 4.3 $\alpha_g = 25^\circ$, plain leading edge

Fig 14 shows the distribution of the total head deficit in the wake of the wing for an incidence $\alpha_g = 25^\circ$. The wake is very large and the maximum numerical value of $|(H - H_0)/q_0|$ is less than at the lower incidence $\alpha_g = 14^\circ$ (Fig 10). Clearly there has been a dramatic change in the flow over the wing during the change of incidence from $14^\circ$ to $25^\circ$; also the wake behind the model support strut (near Y = 500 mm) is much broader. It is not surprising therefore that the areas bounded by the zero contours of the streamwise component of vorticity shown in Fig 15 are similarly enlarged and that the absolute values of vorticity are reduced.

At this incidence it is clearly not possible to associate certain parts of the wake with strake and tip vortices (see also Fig 6c at $\alpha = 22^\circ$) and so, for ease of calculation of the circulation, the large area of positive vorticity in Fig 15 has been divided into two ($Y \leqslant 460$ mm and $Y \geqslant 460$ mm). These areas are shown in Fig 16a together with their associated values of circulation. Fig 16b shows that in the narrow wake $\Gamma(Y)/U_0\bar{c}$ is negative for all values of Y (as it is for $\alpha_g = 14^\circ$) and this is due to the very large spanwise component of velocity as the flow leaves the upper surface at the trailing edge (see Fig 6c).

One interesting point to note is that despite the diffuse distribution of vorticity in this wake, addition of the component values of circulation in the wake gives a total value of $\Gamma/U_0\bar{c}$ of 1.1339 which is almost double that at $\alpha_g = 14^\circ$ (0.5726).

## 4.4 $\alpha_g = 14^\circ$, leading-edge slat deployed

Fig 17 shows the distribution of the total head deficit in the wake of the wing/strake configuration at an incidence $\alpha_g = 14^\circ$ with the leading-edge slat deployed outboard of the strake. The distribution and value of $(H - H_0)/q_0$ in the wake of the strake vortex are changed little by the deployment of the slat (*cf* Fig 10), but below the wake of the strake vortex there is a larger area of low deficit. However, comparison of Figs 10 and 17 shows that the wakes behind the outboard part of the wing are quite different. With the slat deployed, conventional swept-wing attached flow exists, Fig 6d, and a distinct tip-vortex wake can be seen. Between the wakes of the tip and strake vortices, the wake is narrower with the slat on and the waviness in it is probably due to the three slat support brackets the positions of which are shown in Fig 1.

The distribution of the streamwise component of vorticity is shown in Fig 18. The wake of the strake primary vortex has similar values of $\xi\bar{c}/U_0$ to those shown in Fig 11 ($\alpha_g = 14^\circ$, plain leading edge) and once again there is a concentrated region of negative (clockwise) vorticity below it together with a tongue of weaker negative vorticity wrapped around its outboard side.

In the main tip vortex (positive $\xi\bar{c}/U_0$) there is once again a region of contra-rotating flow (negative $\xi\bar{c}/U_0$) (*cf* Fig 8). As before this is attributed to the shedding of a second vortex from the wing upper surface at or close to the square cut wing tip (see section 4.1). Inboard of the wing tip there are local maxima of $\xi\bar{c}/U_0$ which coincide with the waviness of this part of the wake mentioned above. Since the slat support brackets have a bluff square section it is probable that they cause this non-uniformity of the wake.

For this configuration, the distribution of circulation in the wake is shown in Fig 19. Fig 19a shows that the circulation in the strake vortex region is very similar to that for the configuration with the plain leading edge, Fig 12, though that in the tongue is approximately halved. The spanwise distribution of circulation in the narrow wake behind the wing, Fig 19b, is similar in form to that shown in Fig 9 ($\alpha_g = 7^\circ$, plain leading edge) in that it has a peak positive value near $Y = 400$ mm and decreases to zero at the wing tip. This is because the deployed slat at this higher incidence maintains conventional attached flow over the outboard part of the wing.

Since the local velocity vectors for the two configurations at an incidence $\alpha_g = 14^\circ$ have been determined outboard of different spanwise stations (because of a limitation on tunnel time) it is not sensible to sum the circulation components in Figs 12 and 19 for comparison. What can be sensibly done however is to sum the circulation components outboard of the strake vortex and its associated tongue of negative vorticity. For the configuration with the plain leading edge, this gives $\Gamma/U_0\bar{c} = 0.43$ whereas with the slat deployed it equals 0.36 - a reduction in $\Gamma/U_0\bar{c}$ of 0.07, suggesting that the slat causes a reduction in lift (as shown by the force measurements presented in Fig 3). In fact, simple approximate integrations, slat off and slat on, of the circulation in the wake outboard of the strake vortex and its tongue yield a reduction in lift very close to that shown in Fig 3, *ie* $\Delta C_L \approx -0.03$. This suggests that deployment of the slat does not significantly affect the flow inboard of it.

## 5 CONCLUDING REMARKS

The tests described in this Report have provided detailed information about the flow field in a plane normal to the free-stream flow just downstream of a swept wing fitted with a leading-edge strake and with either a plain leading edge or deployed slat outboard of the strake. The data have been analysed to produce distributions of the total head deficit and streamwise component of vorticity in the wake at three angles of incidence for the configuration with the plain leading edge and at one incidence for the configuration with the leading-edge slat deployed. The main features of these distributions have been explained and it is hoped that the information will assist in the understanding and mathematical modelling of such flows.

## Acknowledgments

Acknowledgments are due to Mr P.M. Murdin for providing force data and flow-visualisation photographs from tests on the model at RAE Bedford.

Table 1

MODEL GEOMETRY

| | | | |
|---|---|---|---|
| **Wing** | | | |
| Nominal aspect ratio (in plane of wing) | | = | 3.0 |
| Actual aspect ratio (including effect of anhedral) | | = | 2.93 |
| Wing span | | = | 1.4783 m |
| Wing area | | = | 0.7465 $m^2$ |
| Mean chord | | = | 0.50536 m |
| Leading-edge sweep | | = | $40^o$ |
| Thickness/chord ratio | | = | 8% streamwise |
| Taper ratio | | = | 0.38 |
| Anhedral | | = | $12^o$ |
| Twist | $\alpha_w$ | = | $\tan^{-1}(-0.02527(\eta - 0.226)c_0/c)$ and is applied about the quarter-chord line of the wing |
| Pitching moment datum | | : | ¼-chord point of the zero twist section ($\eta$ = 0.226) |
| **Strake (Strake 2 of Ref 1)** | | | |
| Area (2 off) | | = | 0.05541 $m^2$ |
| Span | | = | 0.3161 m |
| Leading-edge sweep | | = | $75^o$ |
| Leading-edge profile | | : | sharp |
| **Leading-edge slat** | | | |
| Chord | | = | 0.18 c |
| Deflection | | : | $25^o$ streamwise |

Table 2

TEST CONFIGURATIONS

$U_0$ = 50 m $s^{-1}$ for all wake surveys

Configuration 1: Strake and plain leading edge

| | | | |
|---|---|---|---|
| $\alpha_g$ = | 7° | 14° | 25° |
| Number of points in traverse = | 1700 | 1500 | 900 |
| Grid : | 10 mm plus intermediate points in vortices and viscous wake | 10 mm | 20 mm |

Configuration 2: Strake and slat deployed

| | |
|---|---|
| $\alpha_g$ = | 14° |
| Number of points in traverse = | 1700 |
| Grid : | 10 mm |

## LIST OF SYMBOLS

| | |
|---|---|
| $A$ | aspect ratio |
| $c$ | local wing chord |
| $\bar{c}$ | wing mean chord |
| $H$ | local total head |
| $H_0$ | total head in the undisturbed stream |
| $q_0$ | $= \frac{1}{2}\rho U_0^2$ - freestream kinetic pressure |
| $s$ | wing semispan |
| $U_0$ | freestream velocity |
| $X,Y,Z$ | rectangular cartesian coordinates: X positive downstream from the wing tip, Y positive to starboard from the model centreline, Z positive upwards from the wing tip |
| $C_L, C_D, C_m$ | lift, drag and pitching moment coefficients |
| $\alpha$ | model incidence corrected for tunnel constraint |
| $\alpha_g$ | model geometric incidence |
| $\rho$ | density of air |
| $\eta$ | $= Y/s$ |
| $\xi$ | streamwise component of vorticity |
| $\Gamma$ | circulation |
| $\Gamma(Y)$ | spanwise distribution of circulation in the narrow wake |
| $(H - H_0)/q_0$ | non-dimensionalised total head deficit |
| $\xi\bar{c}/U_0$ | non-dimensionalised streamwise component of vorticity |
| $\Gamma/U_0\bar{c}$ | non-dimensionalised circulation |

## REFERENCES


| No. | Author | Title, etc |
|---|---|---|
| 1 | P.M. Murdin<br>G.L. Riddle | Preliminary results of low-speed tests on a research model of a strike fighter configuration.<br>Part I: The effect of leading-edge strakes on the longitudinal aerodynamic characteristics of the model without high-lift devices and tail unit.<br>RAE Technical Memorandum Aero 1818 (1979) |
| 2 | P.M. Murdin | RAE Technical Memorandum (unpublished) |
| 3 | E.C. Maskell | Progress towards a method for the measurement of the components of the drag of a wing of finite span.<br>RAE Technical Report 72232 (1972) |
| 4 | D.A. Lovell | A development of an automatic wake traverse system for flow field measurements in large low-speed wind tunnels.<br>RAE Technical Report (unpublished) |
| 5 | D.A. Lovell | RAE Technical Report (unpublished) |
| 6 | N.C. Lambourne<br>D.W. Bryer | The bursting of leading-edge vortices - Some observations and discussion of the phenomenon.<br>ARC, R & M 3282 (1961) |

Scale - $\frac{1}{16}$

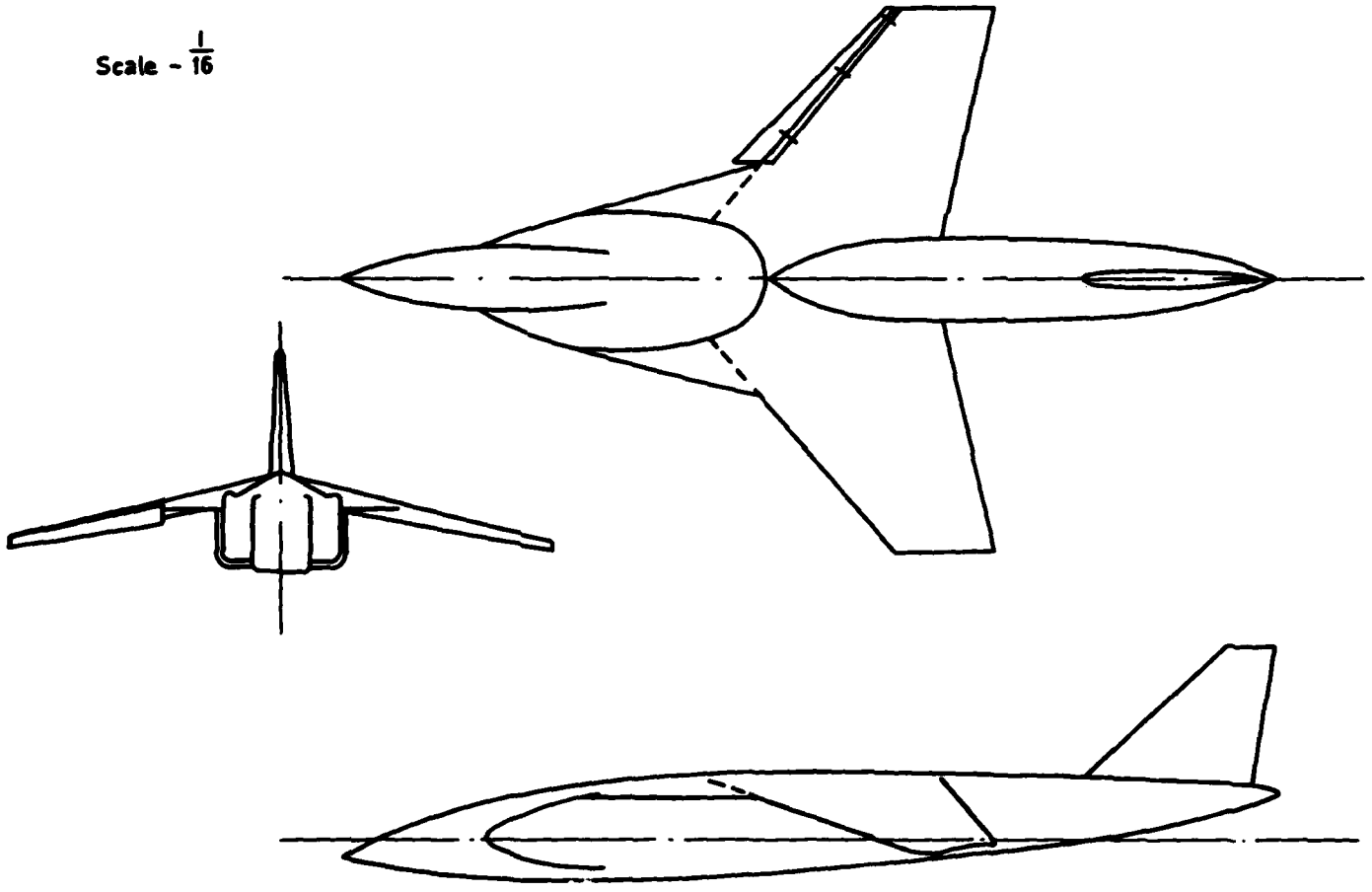

Fig 1 GA of model

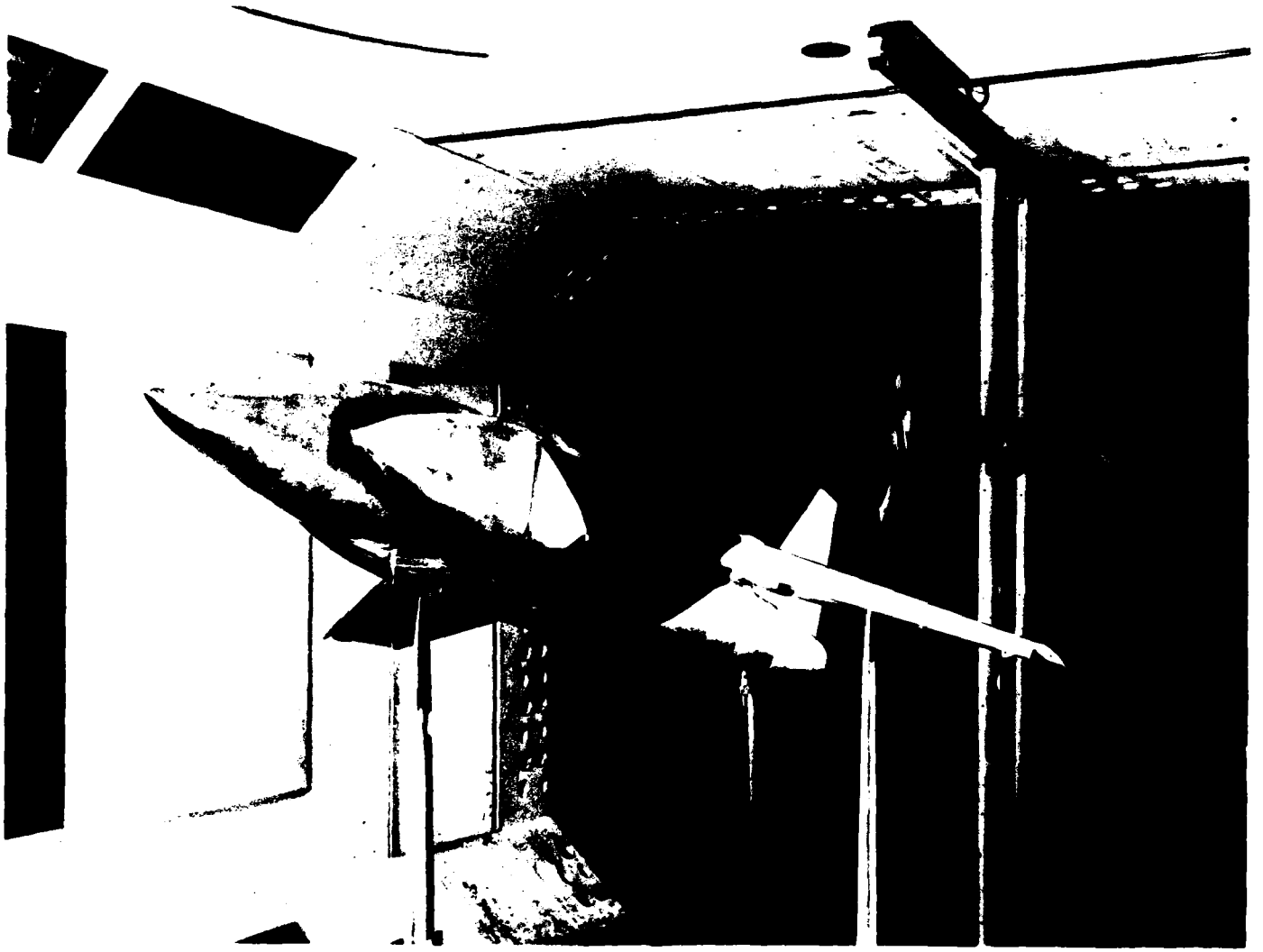

Fig 2 The model mounted in the No.2 11½ft x 8½ft tunnel. Slats deployed, $\alpha_g = 14°$

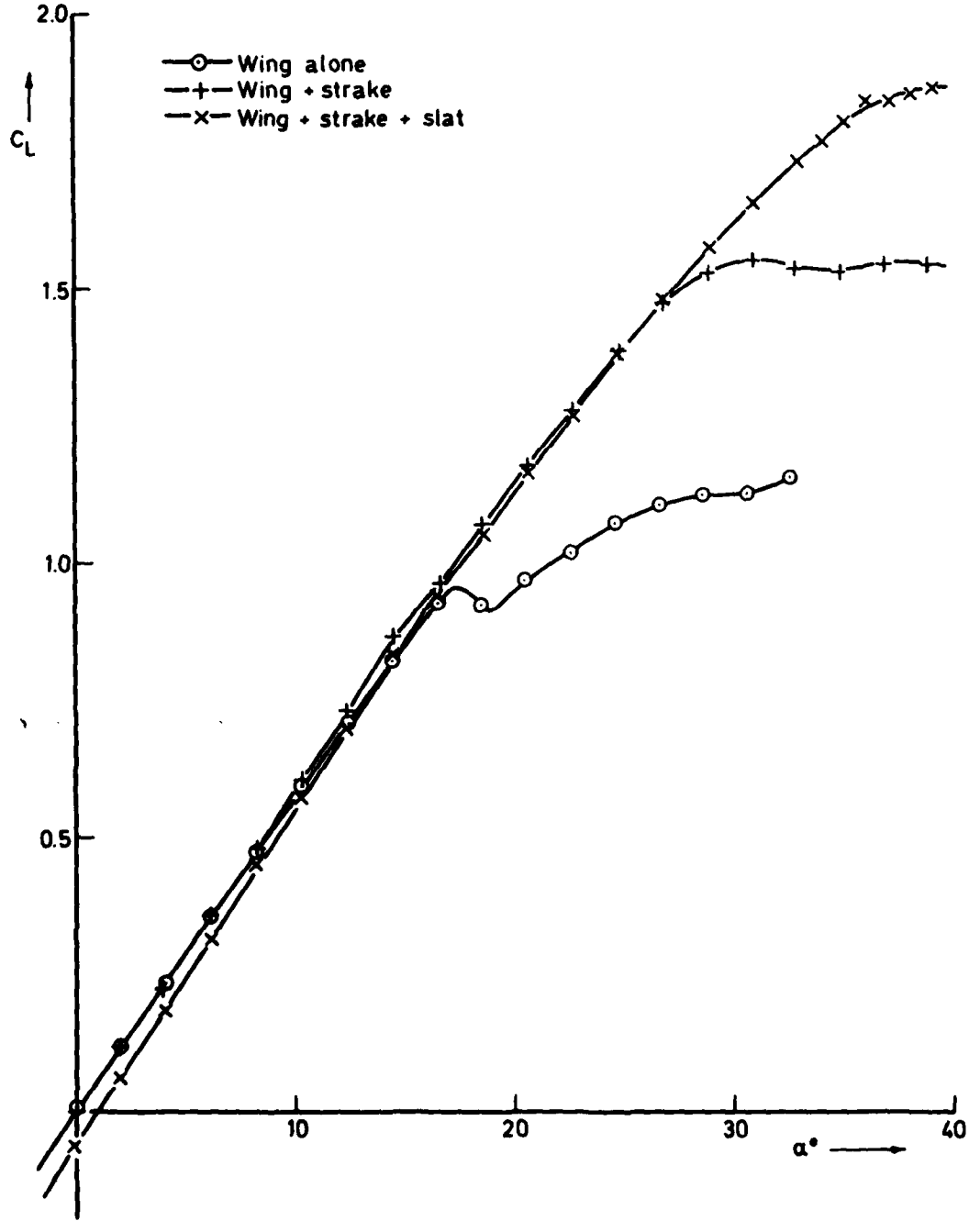


TR 79120

**Fig 3 Longitudinal characteristics, $C_L \sim \alpha$**

Fig 4

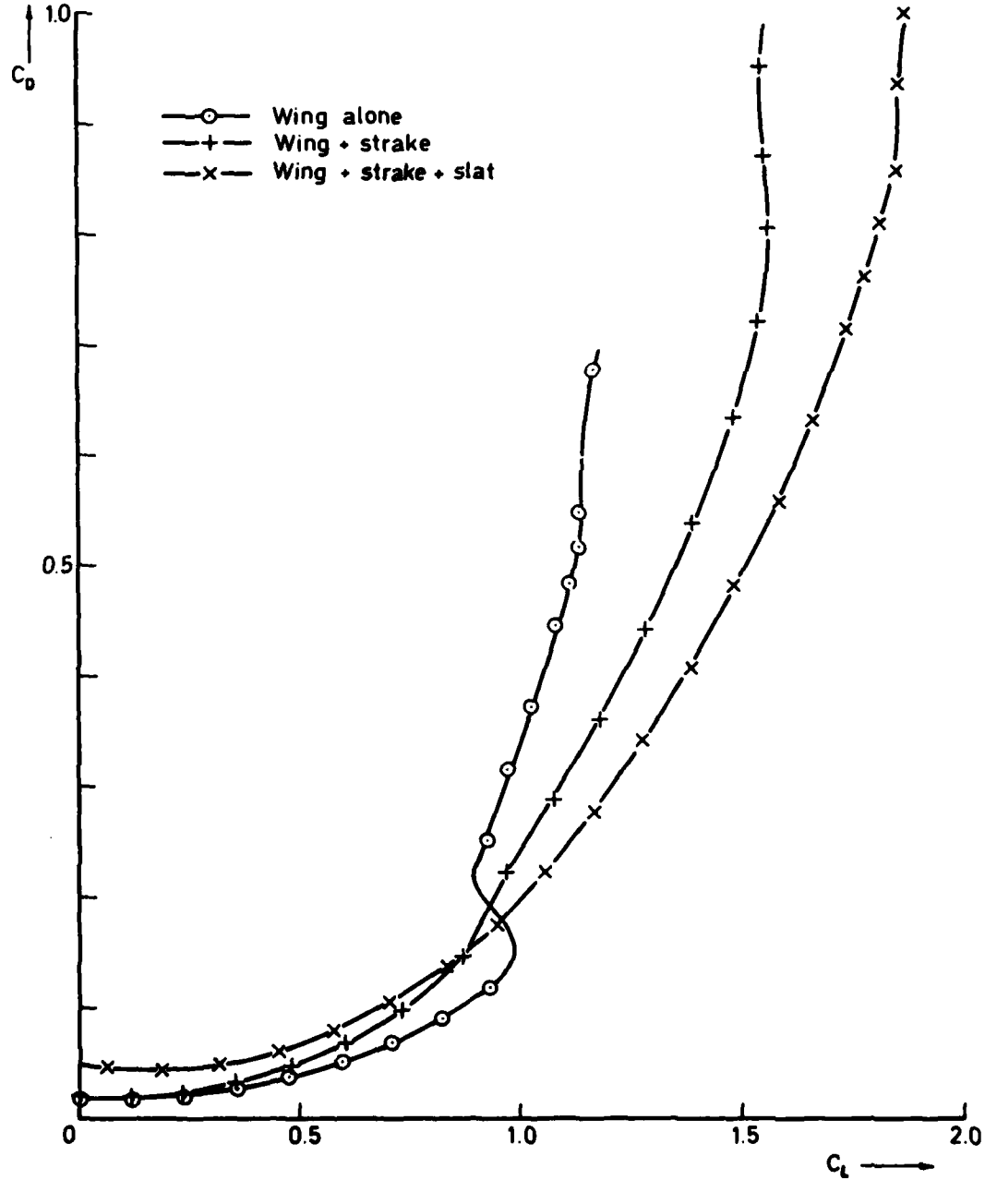


TR 79120

**Fig 4 Longitudinal characteristics, $C_D \sim C_L$**

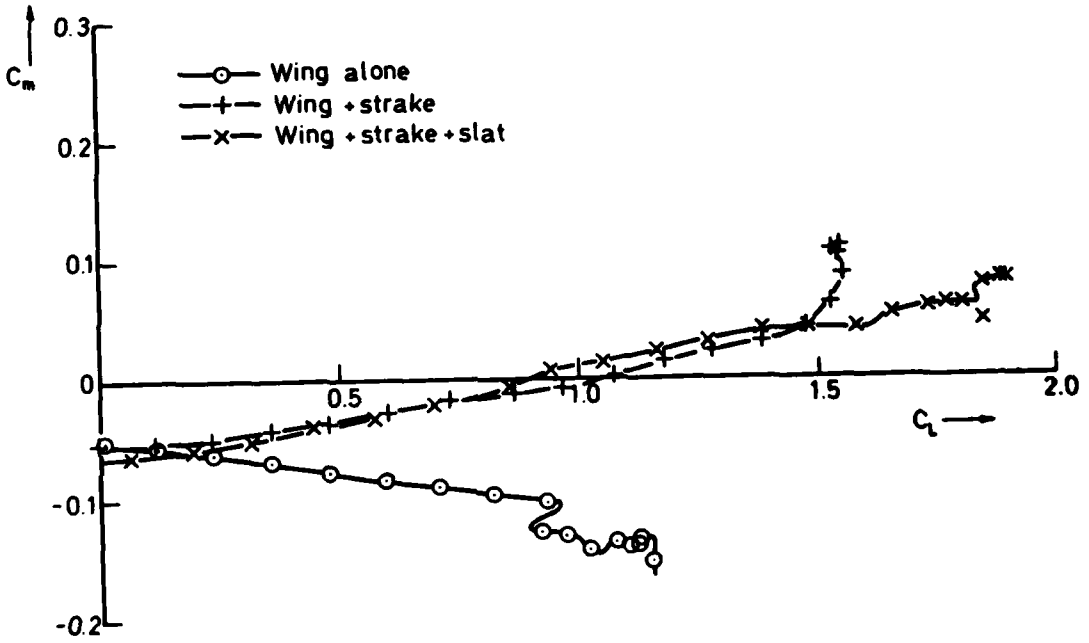


TR 79120

**Fig 5 Longitudinal characteristics, $C_m \sim C_L$**

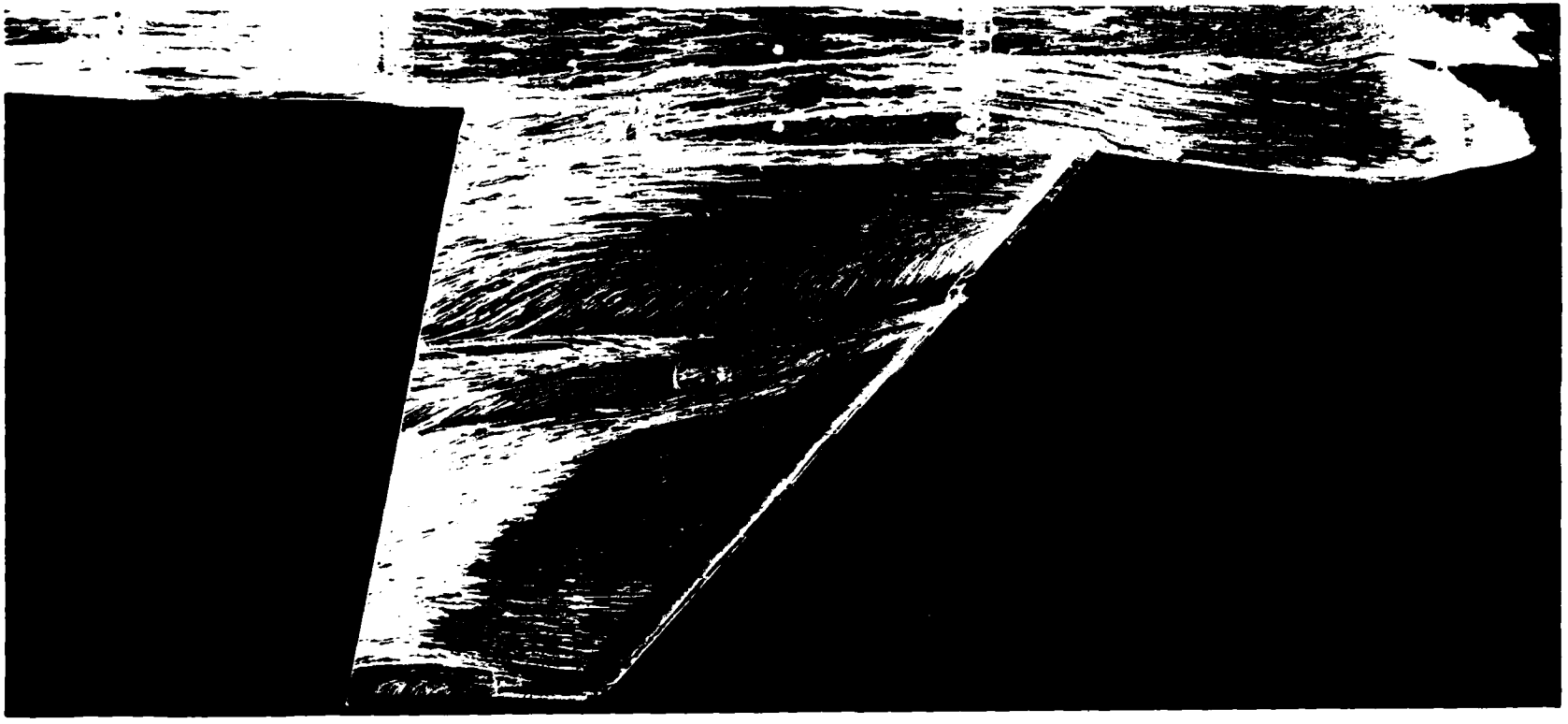

Fig 6a Surface flow pattern, plain leading edge, $\alpha_g = 10°$

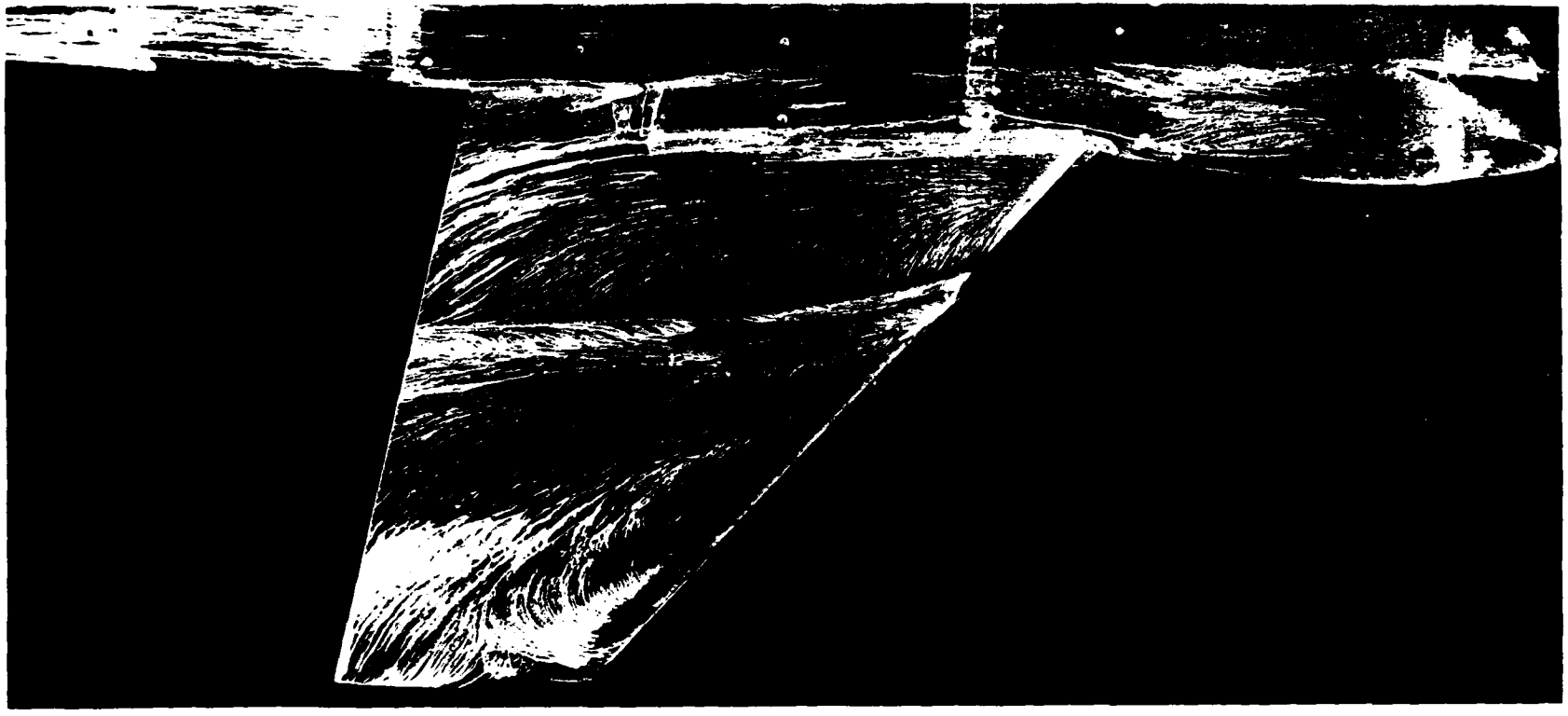

Fig 6b Surface flow pattern, plain leading edge, $\alpha_g = 14°$

Fig 6b

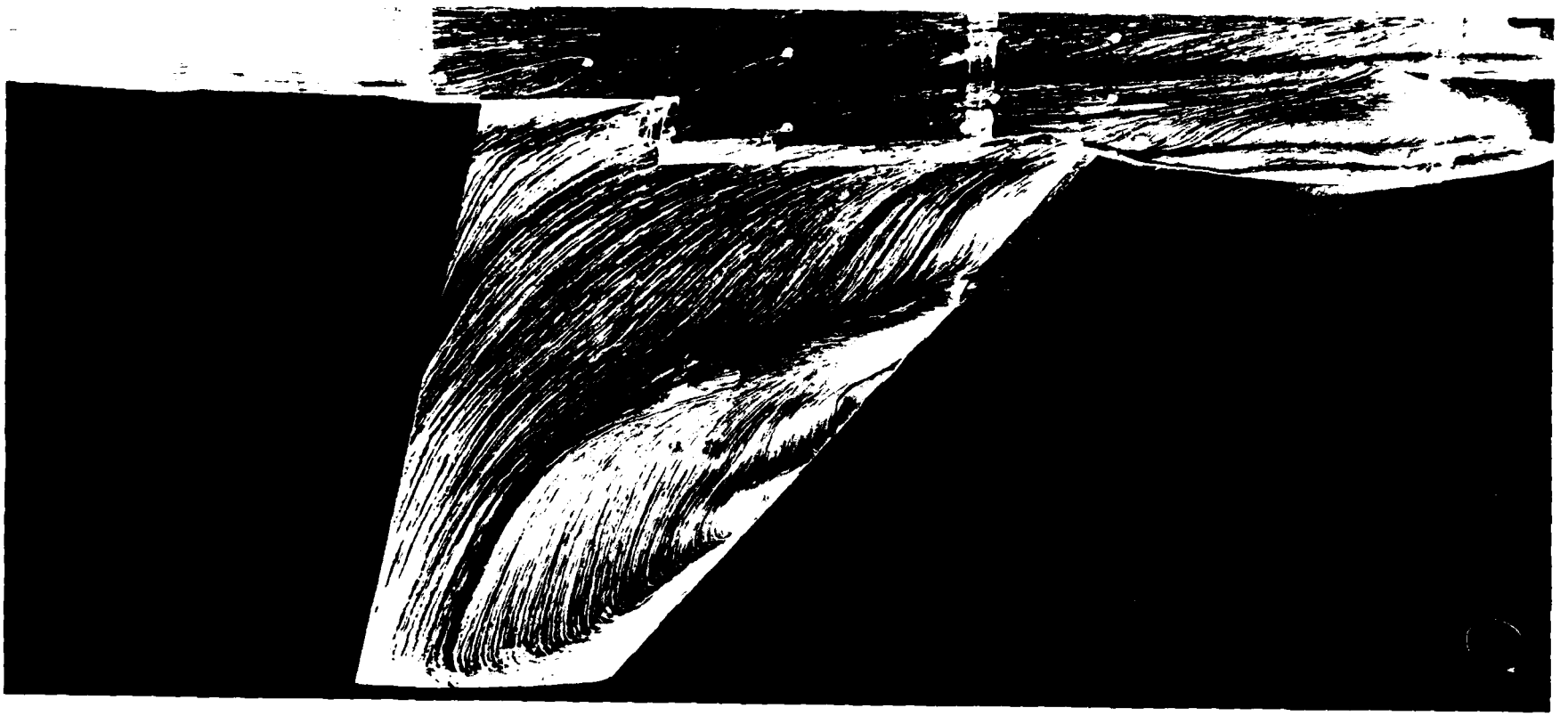

Fig 6c Surface flow pattern, plain leading edge, $\alpha_g = 22°$

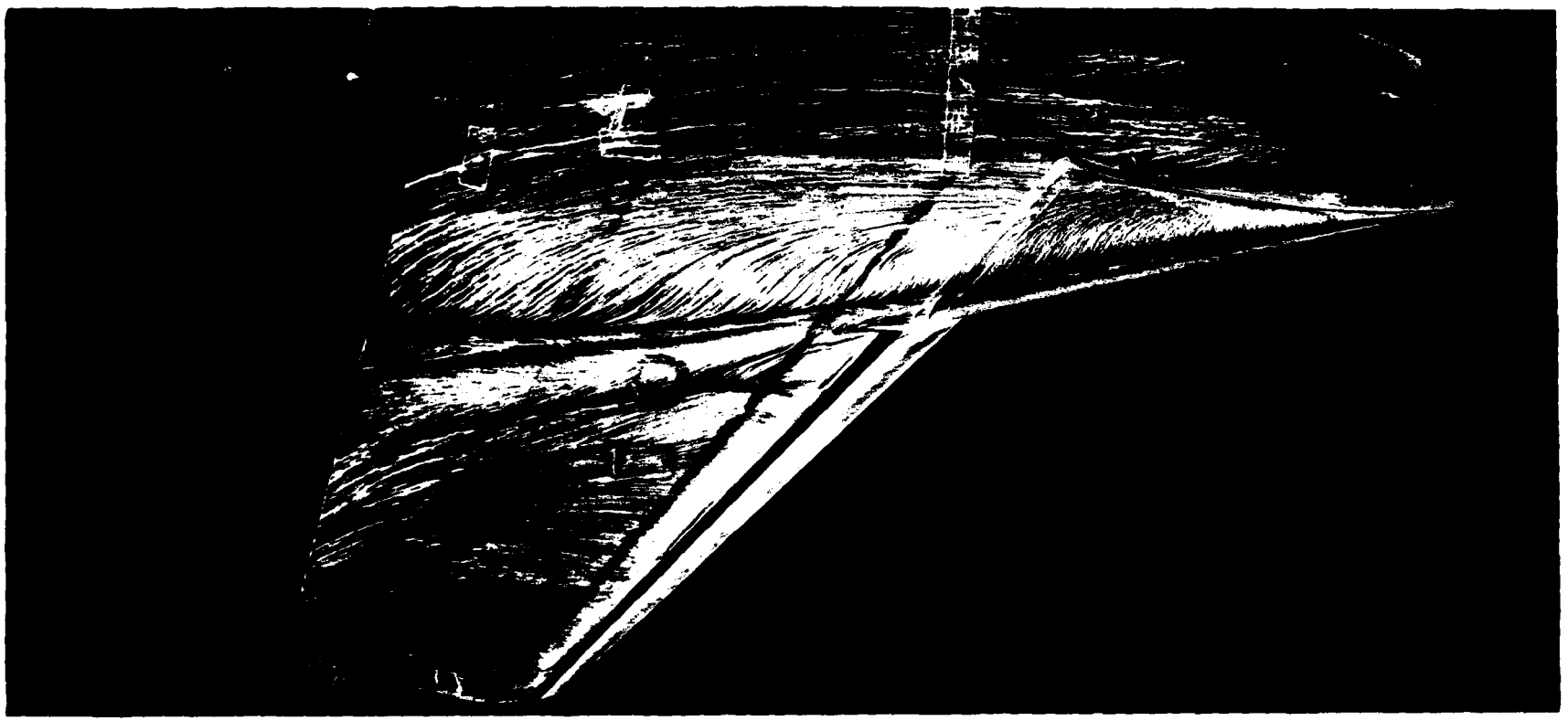

Fig 6d Surface flow pattern, slat deployed, $\alpha_g = 14°$

Fig 7

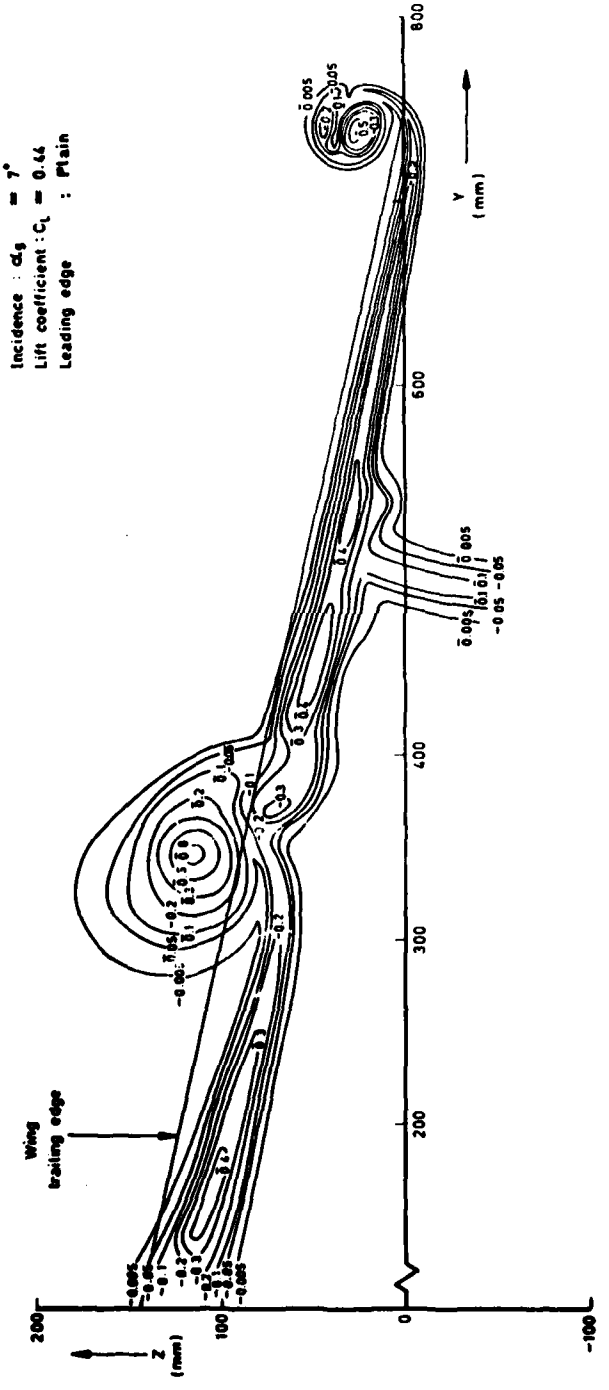


Fig 7 Total head deficit in wake $\frac{H - H_0}{\frac{1}{2}\rho U_0^2}$

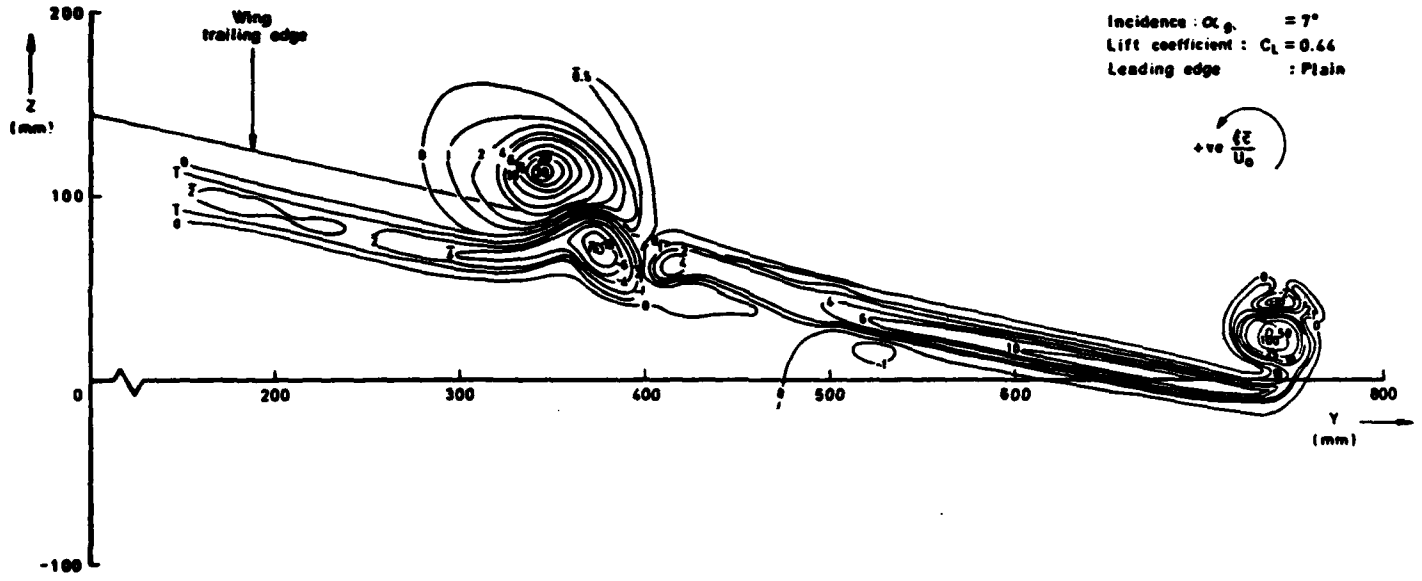


**Fig 8 Distribution of streamwise vorticity component in wake, $\frac{\xi c}{U_0}$**

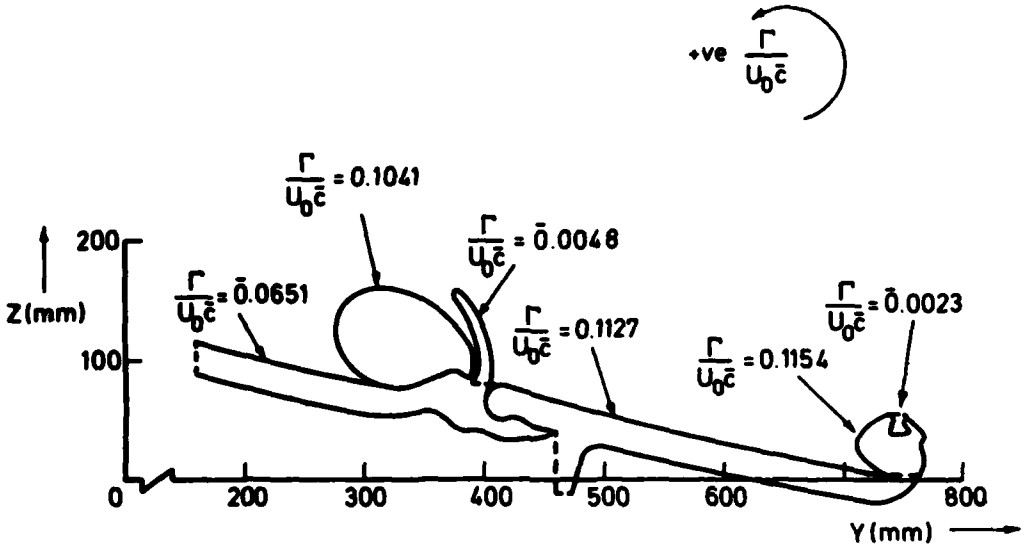


a Circulation components

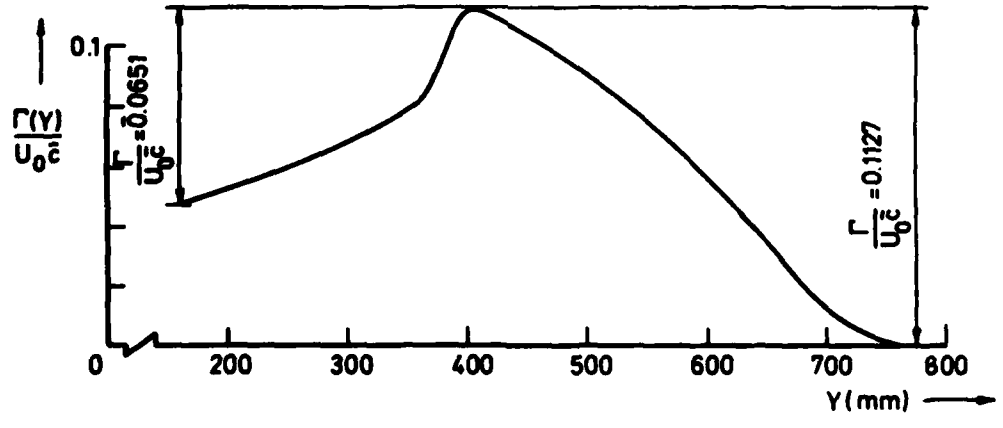


b Circulation distribution in the narrow wake

TR 79120

Fig 9a&b Distribution of circulation, $\alpha_g = 7°$, plain leading edge

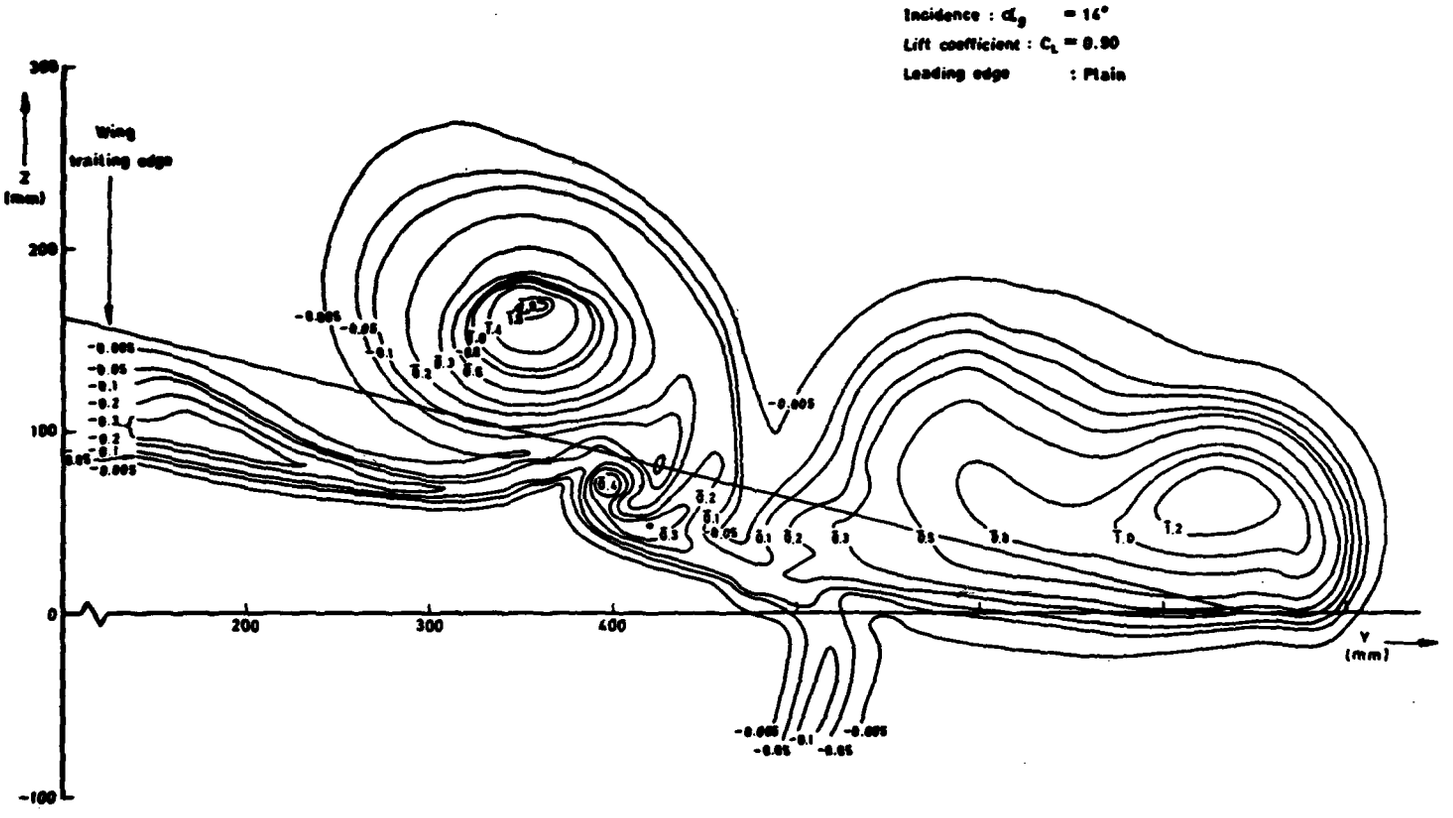


Fig 10 Total head deficit in wake, $\frac{H - H_0}{\frac{1}{2}\rho U_0^2}$

Fig 11

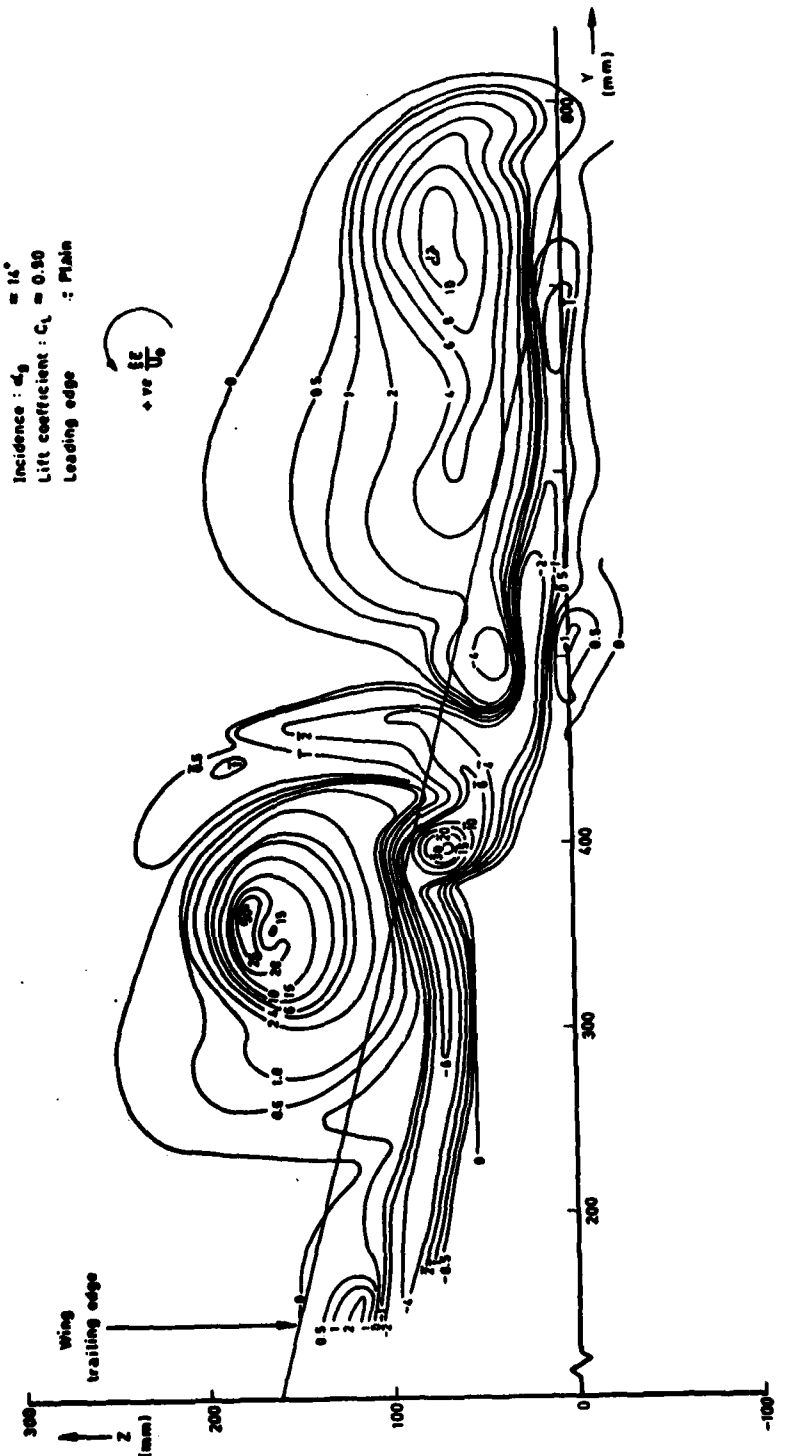


Fig 11 Distribution of streamwise vorticity component in wake, $\frac{\xi\bar{c}}{U_0}$

TR 79120

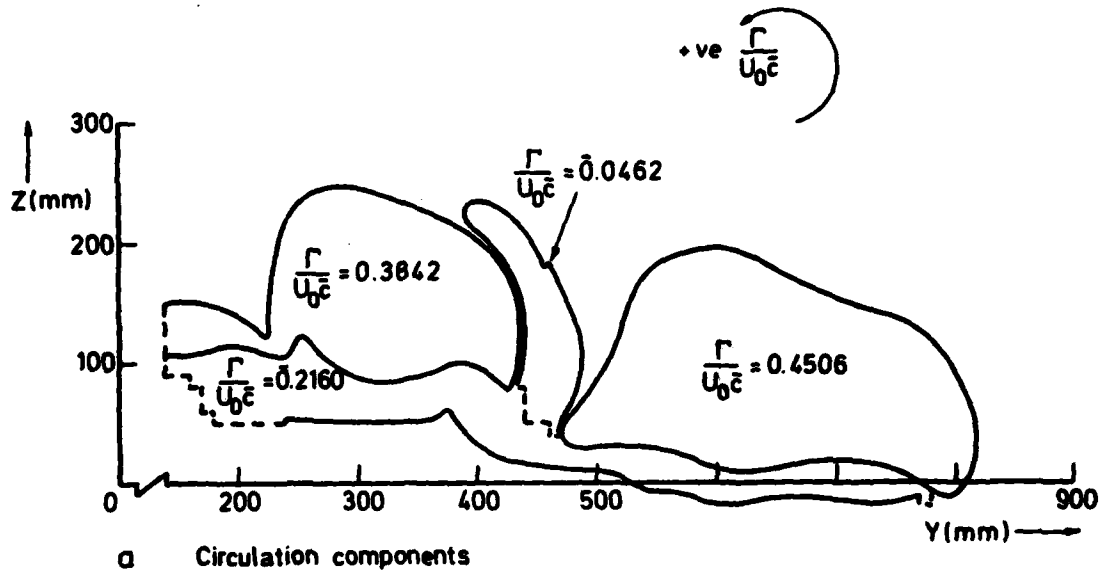


a Circulation components

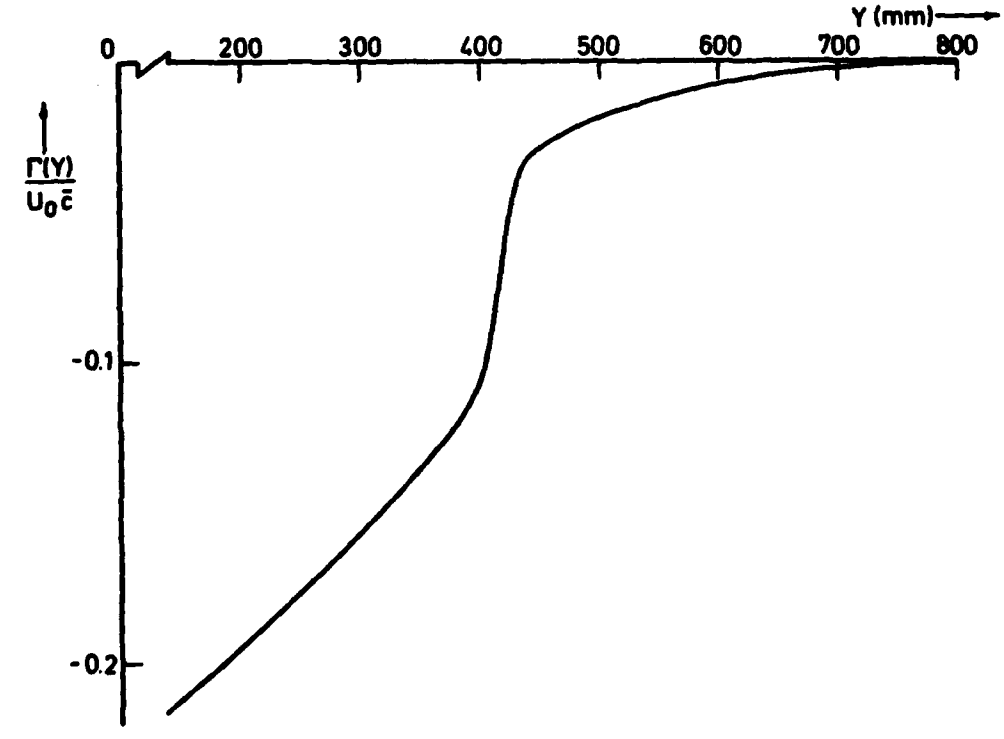


b Circulation distribution in the narrow wake

TR 79120

Fig 12a&b Distribution of circulation, $\alpha_g$ = 14°, plain leading edge

Fig 13

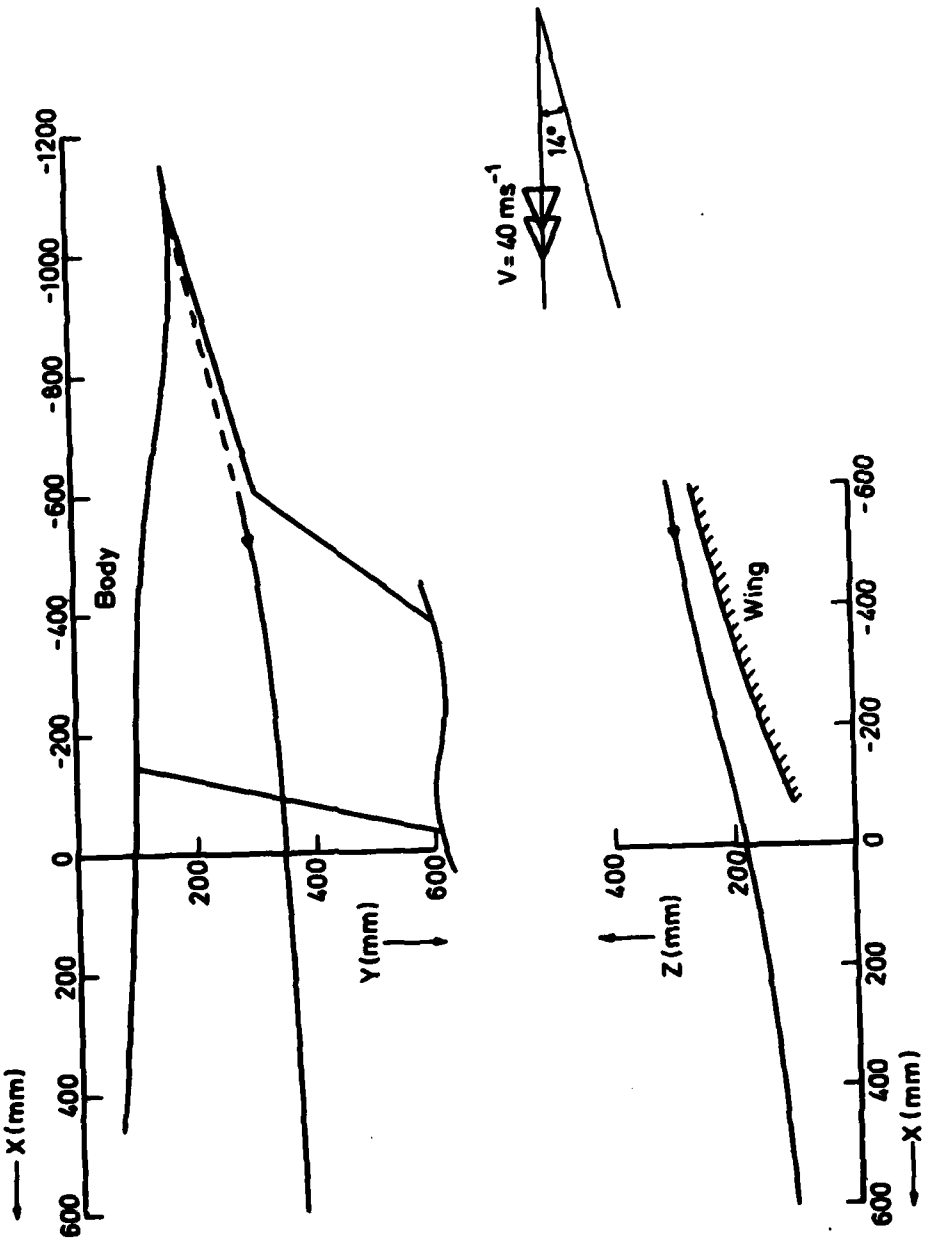


Fig 13 Trajectory of strake vortex, $\alpha_g = 14°$, plain leading edge

TR 79120

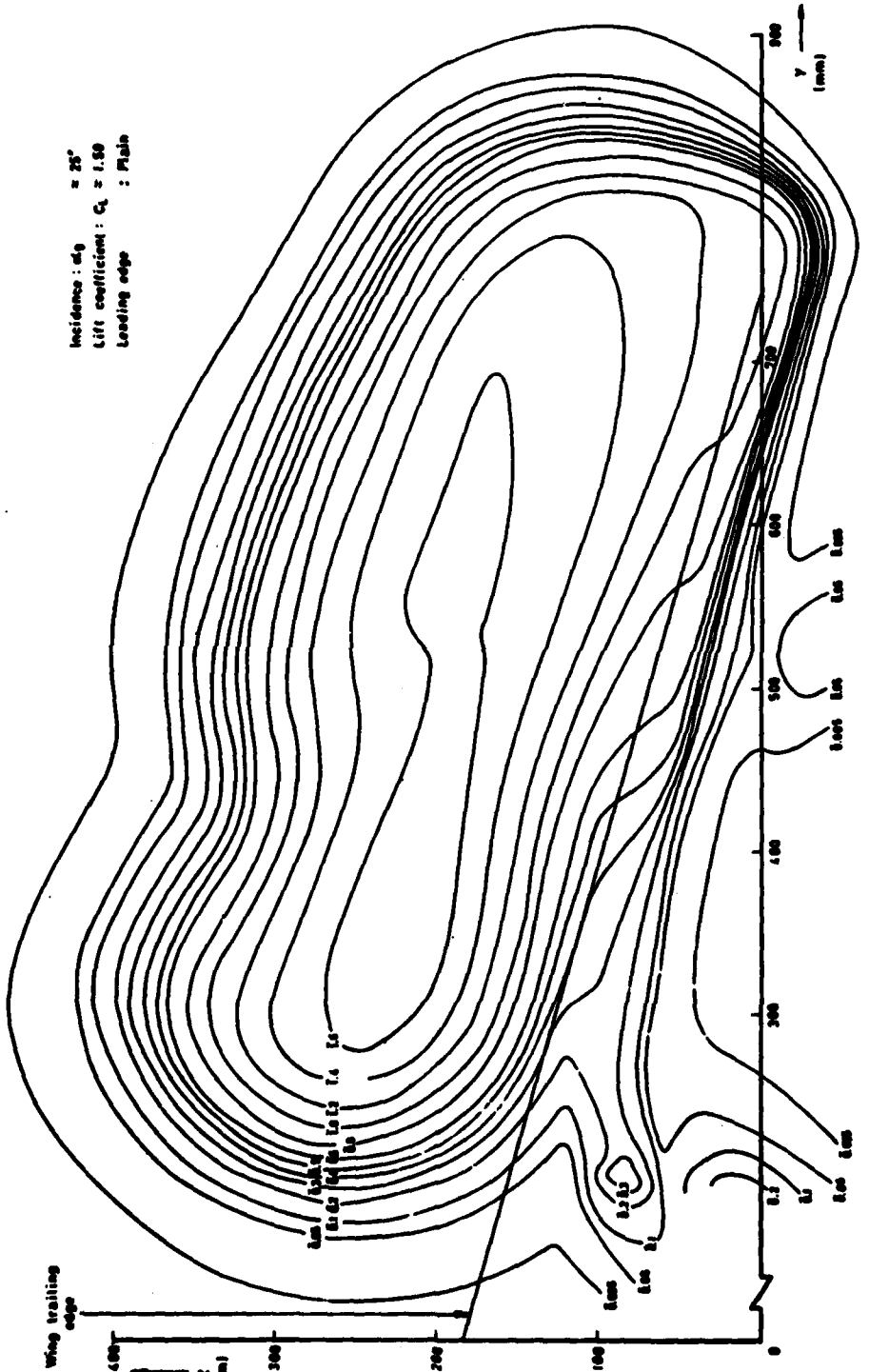


Fig 14 Total head deficit in wake, $\frac{H - H_0}{\frac{1}{2}\rho U_0^2}$

Fig 15

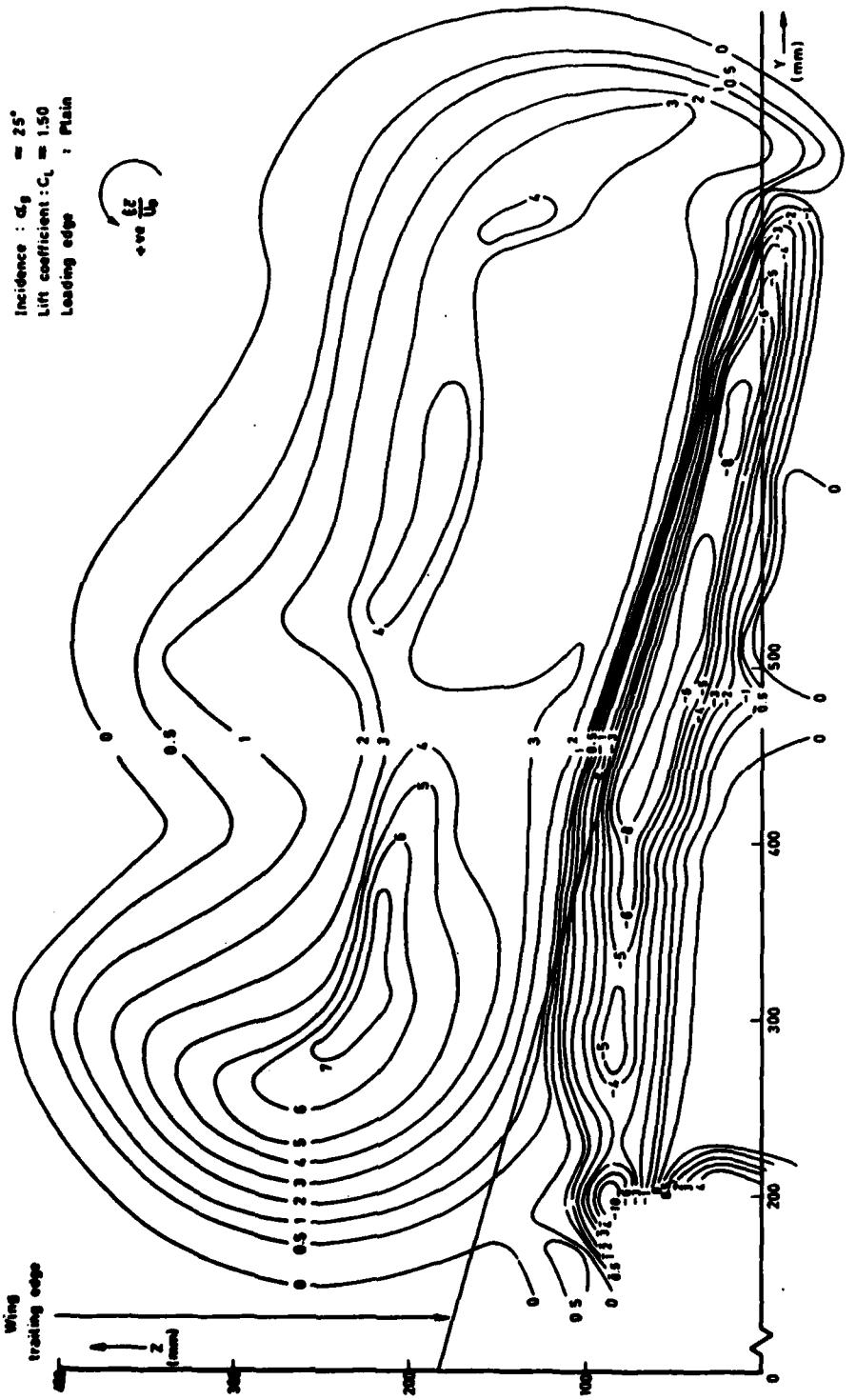


Fig 15 Distribution of streamwise vorticity component in wake, $\frac{\xi\bar{c}}{U_0}$

TR 79120

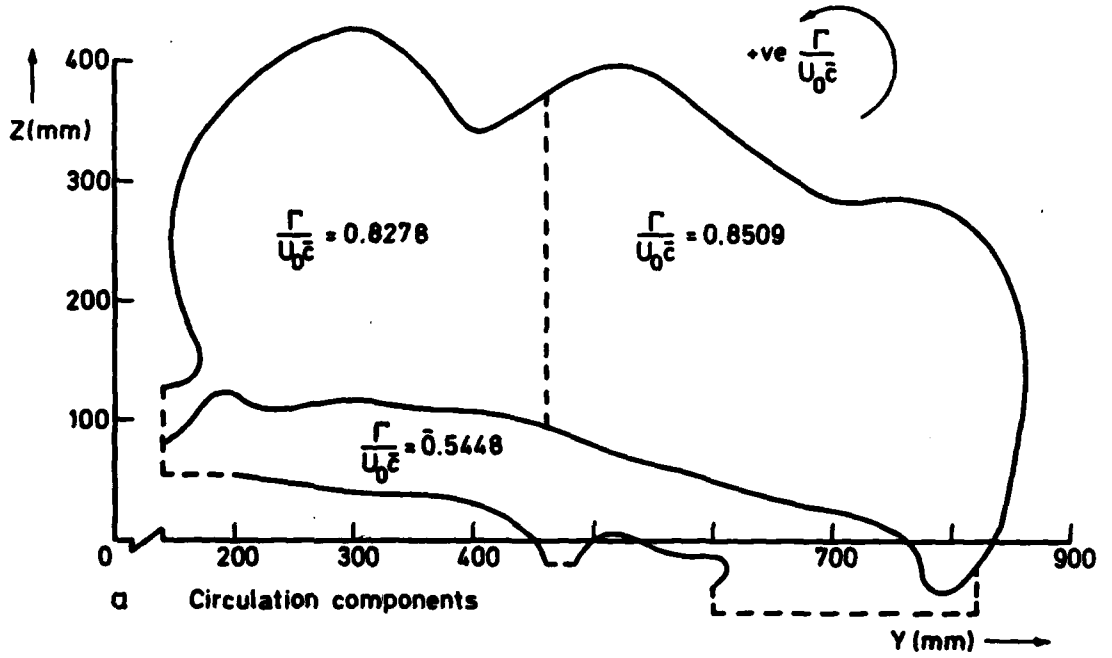


a Circulation components

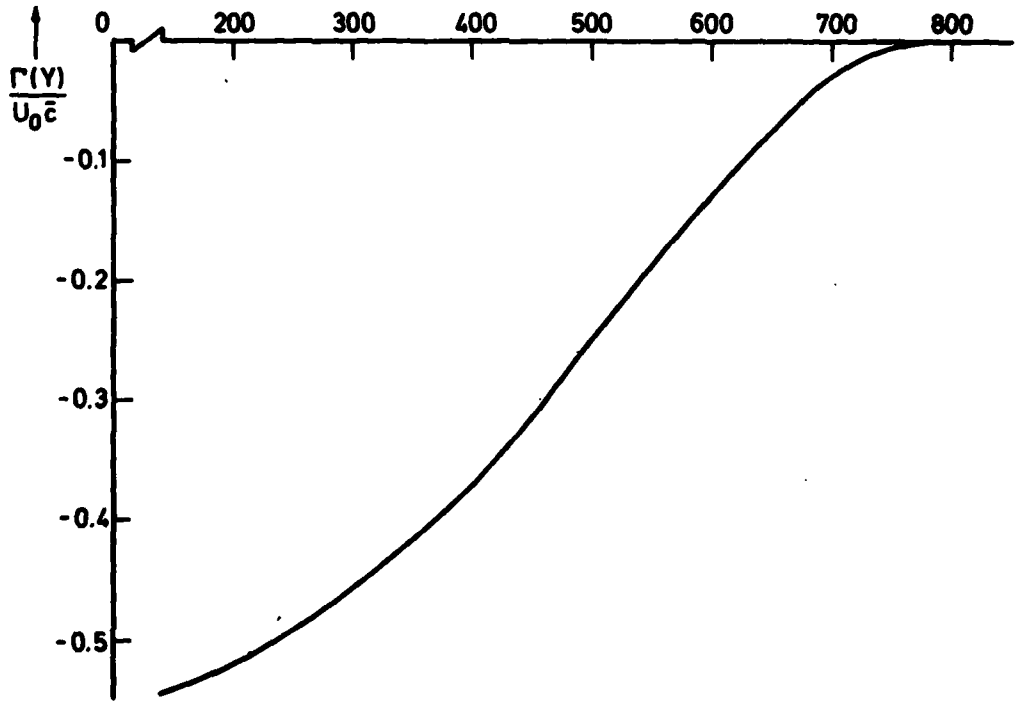


b Circulation distribution in the narrow wake

Fig 16a&b Distribution of circulation, $\alpha_g = 25°$, plain leading edge

Fig 17

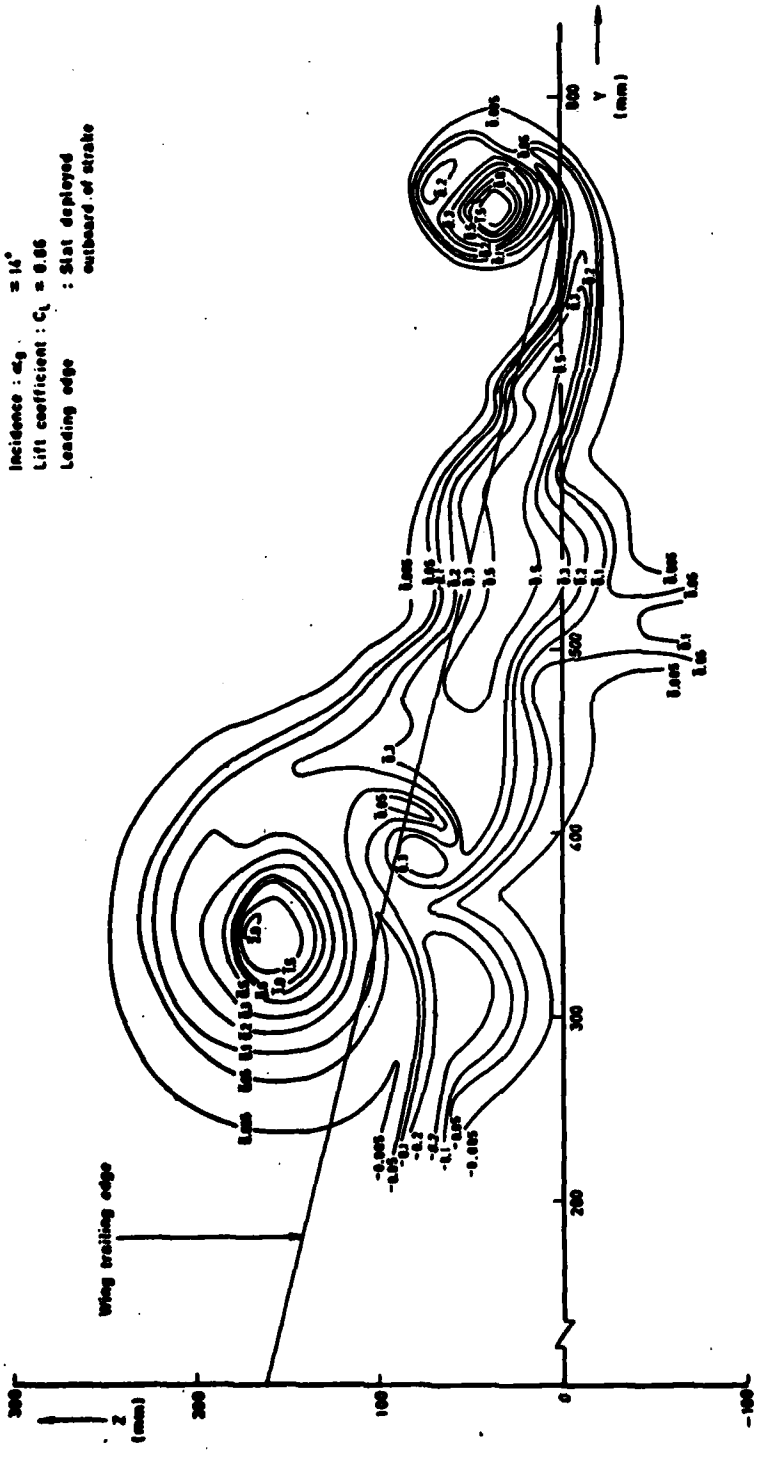


Fig 17 Total head deficit in wake, $\frac{H - H_0}{\frac{1}{2}\rho U_0^2}$

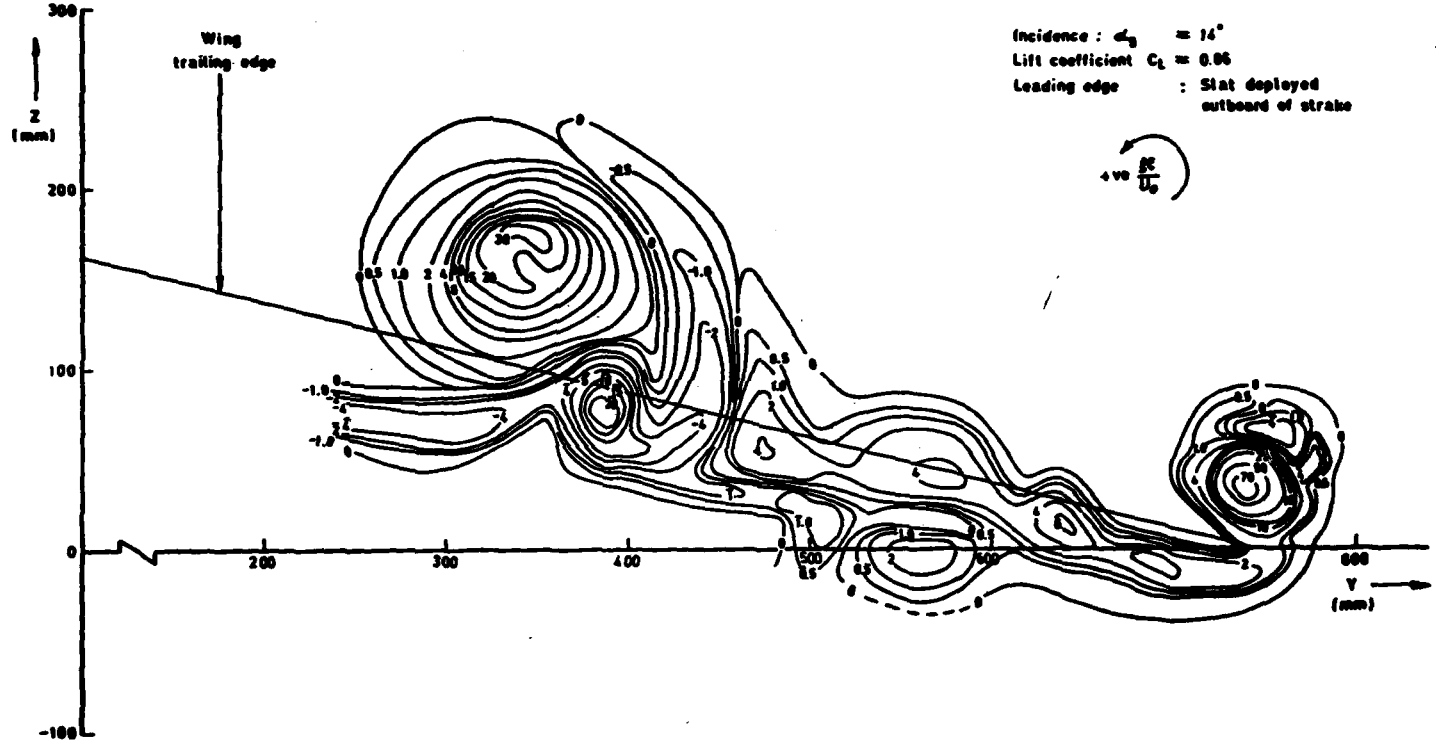


**Fig 18 Distribution of streamwise vorticity component in wake, $\frac{\xi c}{U_0}$**

Fig 19a&b

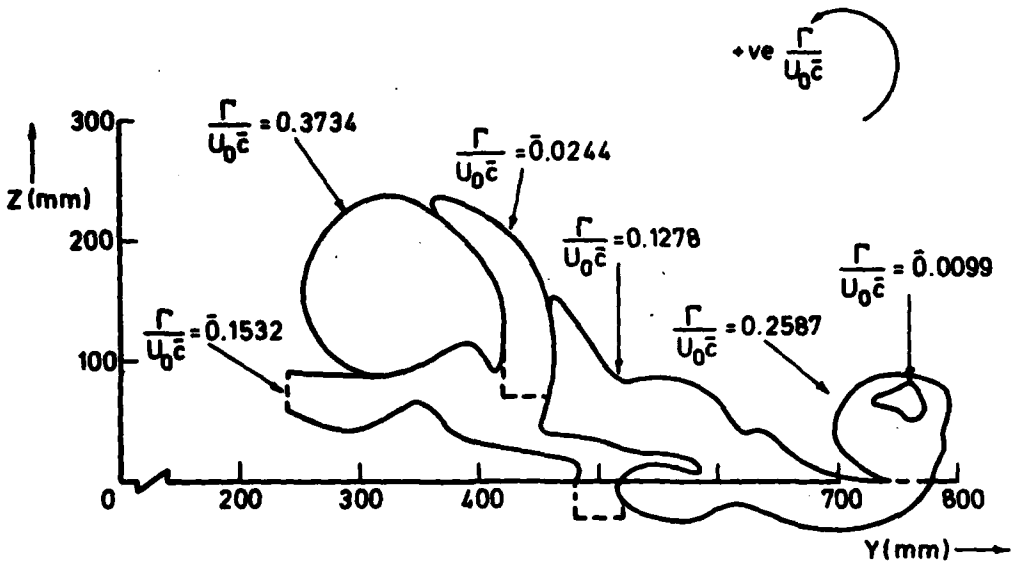


a Circulation components

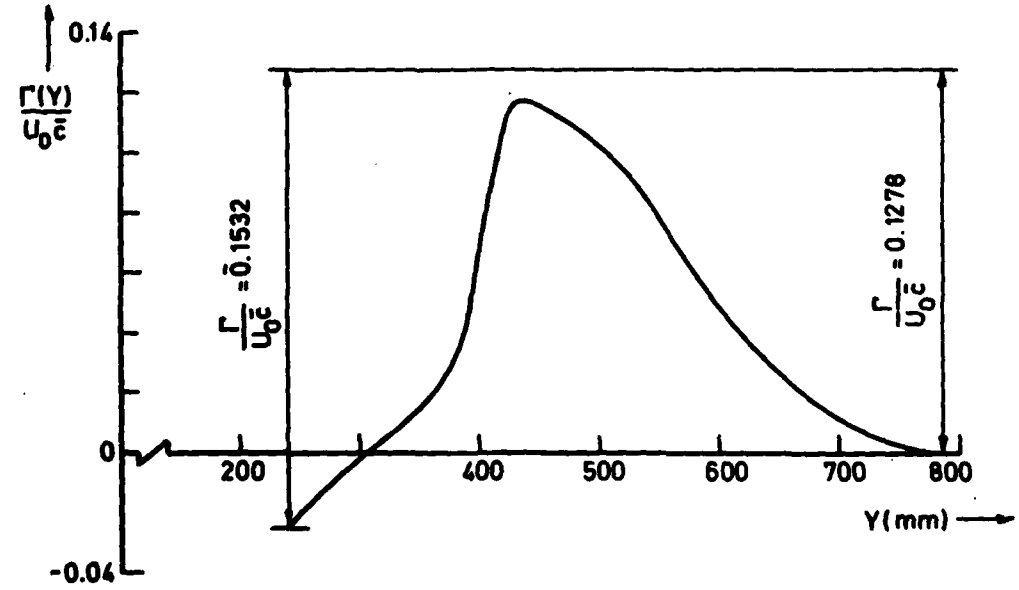


b Circulation distribution in the narrow wake

Fig 19a&b Distribution of circulation, $\alpha_g$ = 14°, leading edge slat deployed

TR 78120

UNLIMITED

| | | | |
|---|---|---|---|
| | 2. Originator's Reference<br>RAE TR 79128 | 3. Agency Reference<br>N/A | 4. Security Classification of Document<br>UNLIMITED |

| | |
|---|---|
| 5. Originator (Corporate Author) Name and Location<br>Royal Aircraft Establishment, Farnborough, Hants, UK | |
| 5a. Sponsoring Agency's Code<br>N/A | 6a. Sponsoring Agency (Contract Authority) Name and Location<br>N/A |

7. Title: Flow measurements in the wake of a wing fitted with a leading-edge vane (strake).

7a. (For Translations) Title in Foreign Language

7b. (For Conference Papers) Title, Place and Date of Conference

| | | | |
|---|---|---|---|
| 8. Author 1, 2, ... | 9a. Author 2 | 9b. Authors 3, 4, ... | 10. Date: Month: Dec, Year: 1979 \| Pages: 39 \| Refs: 6 |
| 11. Contract Number<br>N/A | 12. Period<br>N/A | 13. Project | 14. Other Reference Nos.<br>Aero 2654 |

15. Distributing Activity (Name and Location)
Head of Aerodynamics Dept

16. Abstract
(Abstract text)

17. Keywords (Descriptors)
(Keywords text)